Physics – Uspekhi **52** (2) 137 – 164 (2009)

REVIEWS OF TOPICAL PROBLEMS PACS numbers: 36.40.Ei, **61.46.–w**, 64.70.Hz

Phase transitions in various kinds of clusters

R S Berry, B M Smirnov

DOI: 10.3367/UFNe.0179.200902b.0147

Contents

Abstract. This discussion examines cluster phase transitions and properties related to those phase transitions. Interpreted in terms of their potential energy surfaces, phase transitions in clusters of dielectric and metal atoms differ. Properties of aggregate states of dielectric clusters vary weakly as functions of temperature, and phase coexistence takes place in a range of conditions around the traditional melting point, where the solid and liquid phases have equal chemical potentials. On contrary, the configurational state of a solid metal cluster may well vary as it is heated, and the phase transition results, at least in part, from electronic coupling, as well as from changes in atomic configuration.

1. Introduction

In many ways, large homogeneous clusters as systems of identical bound atoms are convenient models for bulk atomic systems because clusters include bulk systems when clusters are extended to contain infinite numbers of atoms. On the other hand, a cluster constitutes a specific physical object that can have some properties which differ significantly from those of bulk atomic systems. Perhaps first among these properties is the occurrence of what has been called 'magic numbers' of atoms in solid clusters. Clusters composed of these numbers of atoms exhibit characteristically unusual parameters, e.g., maxima in the binding energies of atoms, in the cluster ionization potentials, in the electron affinities, and in the abundances, as functions of the number of atoms comprising the cluster. Magic numbers of solid clusters are observed as local maxima in mass spectra of clusters [1 – 7], and also appear in photoionization spectra of clusters [8 – 10], and in electron diffraction experiments [11 – 16], although these require a specific analysis [17, 18]. The occurrence of magic numbers of cluster atoms is a prime reason for the nonmonotonic dependence of these parameters on cluster size, such as in the case of the cluster melting point. The reason for these is structural — magic numbers correspond to closed shells, either of atoms or of electrons.

Another specific property of clusters is the coexistence of their phases in a range of temperature and pressure in the vicinity of the 'melting point', namely, the set of points at which the free energy of liquid and solid forms are precisely equal. This is a specific property of systems comprising relatively small numbers of atoms or molecules. It was discovered first from computer simulations of Lennard-Jones clusters [19 – 22] and soon thereafter was interpreted and explored further [23 – 28] for Lennard-Jones clusters with completed atomic shells. This phenomenon involves the cluster passing back and forth in some random fashion between (or among) different phase-like forms, so that, if only solid and liquid phases are involved, part of time the cluster spends in the solid state and the rest of the time it resides in the liquid state. Phase coexistence in the vicinity of the phase transition is the universal property of small atomic systems. This coexistence is a consequence both of the time

R S Berry Department of Chemistry, University of Chicago,
929 East 57th St., Chicago, IL 60637, USA
Tel. (01) 773 702 7021. Fax (01) 773 834 4049
E-mail: berry@uchicago.edu
B M Smirnov Institute for High Temperatures,
Russian Academy of Sciences
Izhorskaya ul. 13/19, 127412 Moscow, Russian Federation
Tel./Fax (7-499) 190 42 44
E-mail: bmsmirnov@gmail.com

Received 24 July 2008, revised 27 October 2008
Uspekhi Fizicheskikh Nauk **179** (2) 147 – 177 (2009)
DOI: 10.3367/UFNr.0179.200902b.0147
Translated by R S Berry; edited by A Radzig

scale for passage of a small system from one relatively stable form to another, and of the relatively small difference between the free energies of the favored and unfavored states when the temperature and pressure approach but do not precisely reach the condition making the free energies equal. The free energy difference, in turn, is dominated by the relatively small entropy change in the phase transition, which makes that a key quantity for description of the cluster phase transitions.

We can treat clusters as specific objects, much like molecules, with specific compositions and properties or, alternatively, we can treat them as small, i.e., atomic-scale, models from which we can build an understanding of the properties of bulk, macro-scale matter. It is useful, of course, to do both. We begin by pursuing the second course, and lay the groundwork for interpreting the nature of bulk phase transitions on the basis of the behavior of small systems. Starting from the phase transitions in simple systems of atoms [29 – 32], we divide cluster excitations into thermal and configurational excitations [33], as shown in Section 2.1 for a cluster consisting of 13 atoms. This phase transition is connected in principle with the configurational excitation of atoms, although thermal excitation is also important for the solid – liquid phase transition [32, 34].

Passing from clusters with a simple interaction of atoms (for example, with pairwise atomic interaction) to metal clusters, we add electron excitations to thermal and configurational ones; these may or may not be important in the phase transitions. The electronic spectra of many-particle systems tend to have dense sets of levels, in effect bands of energy levels, rather than very sharp, narrow levels. In truly metallic systems, there is no energy gap between occupied and empty levels, and energy bands with different quantum numbers may overlap. The lack of an energy gap for the electrons and the overlapping of bands can be, in some cases, important for the melting behavior of metal clusters. Here, our goal is to analyze the role of electronic transitions in the phase transitions of metal clusters.

In order to understand the principal peculiarities of the problem under consideration, we consider various limiting cases. We compare metal and Lennard-Jones clusters and consider in detail a cluster consisting of 13 atoms as the smallest cluster with a completed outer atomic shell, and therefore the smallest cluster for which configurational excitation requires a maximum input of specific energy and free energy. In studying the melting transition of this system, we are guided by thermodynamic description as the simplest and most universal method. The possibility of using a thermodynamic description for some cluster behavior simplifies and clarifies the problem. We also make use of other approaches, such as the interpretation of cluster dynamics and kinetics in terms of a potential energy surface. The sum of a comparison of several concepts, models, and approaches for metal and nonmetal clusters allows us to understand various aspects of phase transitions in metal clusters. This is the goal of this paper.

2. Peculiarities of cluster aggregate states and phase transitions

2.1 General principles of cluster evolution

We start from general concepts and models for clusters with a pair interaction of atoms. One can describe such a cluster as a system of bound identical atoms, both in terms of thermodynamics and dynamics. We use classical thermodynamics when we take the interacting atoms to be classical particles. As developed in the 19th century [35, 36], classical thermodynamics deals with concepts of the phase and phase transitions for the atomic system as a whole. For a macroscopic atomic system, the phase or aggregate state of the atomic system is introduced as a uniform spatial distribution of atoms with boundaries, and the phase transition between the aggregate states we call phases has a stepwise character. Transferring from macroscopic atomic systems to clusters consisting of a finite number of atoms, it is necessary to revise this definition, still keeping the concept that thermodynamics reflects the properties of a large ensemble of systems identical with the one we wish to study. The aggregate state is a sum of configurational states (or it may be just one configurational state) with similar excitation energies if this sum of states is realized with a very high probability under suitable conditions [32]. We see that clusters occupy an intermediate position between macroscopic systems and simple systems, atoms or simple molecules. Thermodynamics does not describe simple individual atomic systems but is suitable for describing large collections of them. However, from its inception, thermodynamics was meant principally for the description of macroscopic atomic systems. Although clusters individually are systems of relatively small, finite numbers of atoms, by describing them in terms of Gibbsian ensembles, thermodynamics is entirely adequate and appropriate for their description.

The dynamic description of clusters is based on the methods of molecular dynamics (MD) in which the equations of motion are solved for successive, short time steps. Some questions about the nature of phase transitions in small atomic and molecular systems can be answered on the basis of such calculations, via computer simulations. In particular, simulations help clarify why phase transitions occur in clusters and are absent in individual atoms and molecules, they reveal what and how many aggregate states an atomic system can have; they show the connection between aggregate states and the character (e.g., the range) of atomic interactions. Classical simulations show the spatial and velocity distributions of all the atoms or molecules at each time step, i.e., they provide comprehensive information about cluster's behavior. Only small portion of this information is left over when passing to thermodynamic description but nevertheless most important characteristics of the object are singled out in the process.

Computer simulation of clusters by methods of molecular dynamics is most convenient for a system of atoms with pairwise interactions. Often the Lennard-Jones interaction potential is used for a system of atoms and has the form [37, 38]

$$U(R) = D\left[\left(\frac{R_0}{R}\right)^{12} - 2\left(\frac{R_0}{R}\right)^{6}\right], \qquad (2.1)$$

where R is the distance between atoms, R_0 is the equilibrium distance in the diatomic molecule, and D is the well depth. Although this potential does not describe even compressed inert gases [32, 39, 40] and hence is not related in a fundamental way to real atomic systems, the Lennard-Jones interaction potential may be convenient as a model because it contains simultaneously short-range and long-range parts and gives a reasonably accurate description of many systems, notably systems of rare gas atoms.

The dynamic description of clusters by molecular dynamics gives rich information about their behavior. But it is necessary to extract from this a restricted number of parameters that best characterize the system. One can obtain these through a combination of dynamics and thermodynamics. The basic thermodynamic parameters in a range of phase coexistence are the cluster temperature (or the temperature of the solid and liquid states separately when the cluster is a microcanonical ensemble of atoms), the energy and entropy of the phase transition, the probabilities of cluster residence in the solid and liquid states at a given cluster temperature (or the excitation energy), and the anharmonicity parameter for the solid and liquid states. These parameters allow us to portray the character of cluster evolution in the range of phase coexistence. These data may be enriched by information on the second level that follows from the results of dynamic cluster simulation and includes the average lifetime for each aggregate state at a given temperature, distributions over lifetimes and other cluster parameters, etc. This information gives a more detailed description of cluster behavior.

Such a combination of dynamic and thermodynamic methods of cluster description opens the way for us to understand the microscopic nature of cluster aggregate states. In this way, simulations showed and then led to the understanding of one striking cluster property — the coexistence in clusters of two or more phases over a range of temperature and pressure at melting, instead of phase coexistence only along a sharp curve dividing the regions of stability of the two phases. That the solid – liquid transition is gradual in very small clusters was recognized for small Lennard-Jones clusters by both molecular dynamics [19, 20] and Monte Carlo [21, 22] simulations. A clearer understanding emerged with more extensive simulations which showed that regions of phase coexistence are found for much larger Lennard-Jones clusters [23 – 28]. The phenomenon of phase coexistence follows from the way the equilibrium ratio of the amounts of two phases of a small system remains near enough to unity for the unfavored phase to be present in observable amounts under attainable, measurable conditions somewhat away from the precise temperatures and pressures at which the free energies and chemical potentials of the two phases are precisely equal. This, in turn, is due to the relatively small entropy change in the phase transition for clusters. This transforms a melting point for macroscopic atomic systems into a transition range for clusters and must be the basis for describing the cluster phase transitions.

In contrast to how we first came to understanding phase changes of clusters (and still get the greater part of our knowledge of these systems), our knowledge of the phase transitions in macroscopic systems was gained in a different way. In the case of macroscopic atomic systems, the concepts and validity of the classical thermodynamics of phase transitions and of their thermodynamic parameters resulted from observation and experiment, and thus from corresponding measurements. A particularly vivid example is the Gibbs phase rule relating the number f of degrees of freedom to the number of components c and the number of phases p in equilibrium together: $f = c - p + 2$. (This equation is remarkable insofar as the three variables are almost trivially related, and the one remarkable entry, that can be found only from observation and not by deduction, is the 2.) This knowledge for macroscopic systems obtained within the framework of classical thermodynamics must also be taken into account for clusters with suitable adjustment for the size of this atomic or molecular system.

An important element in the description of dielectric clusters may be the potential energy surface (PES) constructed in a multidimensional space of atomic coordinates. The basis of this concept is the Born – Oppenheimer approximation in which we assume that the electrons of a polyatomic system equilibrate essentially instantaneously with respect to any motion of the nuclei, so that we can associate an internal energy with every possible configuration or structure of the system, independent of the history of formation of this structure. This is particularly useful when all the electronic excitations in the system are larger than the energies associated with atomic motions, so that only a single energy surface need be considered. Therefore, the PES approach is appropriate for describing dielectric clusters but may not be appropriate for some kinds of metals or semiconductors. Next, in considering cluster evolution as changes of atomic coordinates on one PES, we use the adiabatic approximation assuming the PES position to be independent of atomic velocities. This allows us to transfer from a statistical description of atoms in the phase space to accounting for their motion in the coordinate space only.

In the analysis of cluster evolution as a motion along the PES, the topographical properties of the PES are at the essence of the issue. It is important that a PES of any dielectric cluster with pairwise atomic interactions has many local minima [41 – 45]. In particular, for the Lennard-Jones cluster of 13 atoms, the number of geometrically distinct local minima of the PES is on the order of a thousand [41, 47]. Moreover there are approximately $n!$ permutational isomers of any one geometric structure consisting of n atoms [43 – 45, 48, 49]. One can see that the PES description of cluster evolution holds true if a typical atomic energy is small compared to a typical potential barrier height between neighboring local minima of the PES. Then, in the course of cluster evolution, the typical time that a cluster resides near each local minimum is long compared to the time of transition to a neighboring local minimum. This allows one to consider the vicinity of each local minimum as a current configurational state associated with a configurational excitation energy. In this way one can separate the oscillations and configurational degrees of freedom for cluster atoms [33]. This character of cluster evolution provides a basis for the analysis of dielectric clusters.

Barriers between neighboring local minima of PES are relevant to the rates of transition between them, and hence the PES method is easiest to use at zero temperature. At finite temperatures, one must have a more detailed knowledge of the surface topography in order to use that topography in a rigorous way. Nonetheless, even a limited knowledge of a PES can give a qualitative or even a semiquantitative description of transitions among the local minima of the PES. The saddle structure of any PES is a crucial, inherent characteristic for cluster dynamics [43 – 46] because it compels a cluster to spend a relatively long time near each local minimum. Therefore, the dynamics of cluster evolution that proceeds through the transitions between neighboring local minima of a PES is often called 'saddle-crossing dynamics' [47].

2.2 Configurational cluster excitation

We have two forms of atomic excitations in dielectric clusters, thermal vibrational motion and configurational excitation

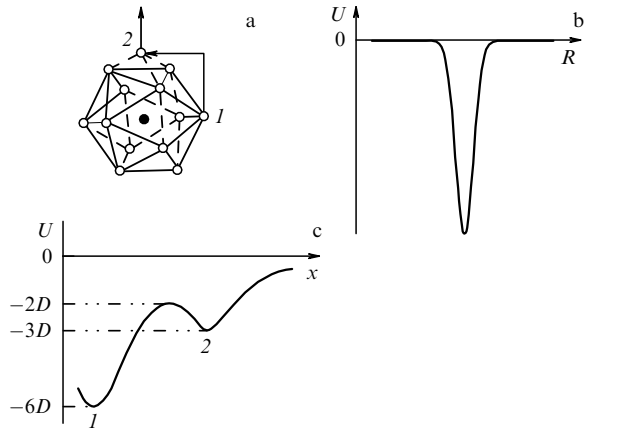

Figure 1. Configurational excitation of a cluster consisting of 13 atoms with a short-range interaction between the nearest neighboring atoms: (a) the character of configurational excitation; (b) the pair interaction potential of the atoms, and (c) the cross section of the potential energy surface along the transition coordinate. Numbers *1* and *2* in Fig. 1a mark stable configurations of atoms that correspond in turn to cluster aggregate states.

that corresponds to a change in the atomic structure of the cluster. Figure 1a demonstrates the lowest configurational excitation of a 13-atom cluster comprising atoms that interact via a short-range pair potential of the kind shown in Fig. 1b. As a result of this excitation, an atom is transferred from the cluster surface (point *1*) to a position above the cluster surface (point *2*) which locates the promoted atom in the potential well created by three surface atoms. Note that a short-range atomic interaction in a cluster means interaction between nearest neighbors, which for a pairwise atomic interaction corresponds to the small well width in Fig. 1b, compared to the distance between nearest neighbors.

Let us analyze the configurational excitation of Fig. 1a in more detail. In this case, the transferring atom has 6 bonds with nearest neighbors in the initial state (at position *1*) and only 3 bonds in the final state (at position *2*). Hence, in ignoring a thermal motion of atoms, the excitation energy equals $3D$, where D is the energy required to break one bond. But in the course of atom transferring, one can preserve only two bonds under optimal transfer conditions. Therefore, this configurationally excited state is separated by an energy barrier between the initial and other states, and the barrier height is $1D$ above the upper minimum and $4D$ above the lower minimum. These energies relate to a short-range interaction. Accounting for an additional long-range interaction and thermal motion of atoms leads to a change in the parameters of configurational excitation and barrier height, but the character of the interrelation between these values will be conserved.

This simple consideration for the 13-atom cluster with a short-range interaction between atoms allows us to describe the character of transitions between configurational states. Along with cluster excitation, an inverse transition is possible for an atomic particle from the cluster surface to an external shell. Then, after some time, another atom transfers from an external shell to its surface. In this manner, an equilibrium is established between the ground and excited cluster configurational states. Thus, the atomic transitions require overcoming a barrier of height $1D$ for atoms with short-range interaction. Correspondingly, motion of a promoted atom over the cluster surface proceeds more easily than transitions between the ground and excited configurational states and even more so in comparison with the exchange of positions of two atoms in the ground configurational state. Hence, relating the cluster's aggregate state with the atomic mobility in this state, we identify the ground configurational state as the solid aggregate state of the 13-atom cluster, and the lower excited configurational state perturbed due to atomic interaction as the liquid aggregate state. The presence of a long-range interaction between atoms does not change this representation so long as the short-range interatomic interaction dominates.

We now look at treating the dynamics of cluster evolution in terms of the PES for this system in the many-dimensional space of atomic coordinates [48, 49]. We have to recognize significant differences between the behavior of metal and dielectric clusters in their evolution along their PESs. Figure 1c exhibits a cross section of the relevant part of a PES when one atom is displaced from the ground configuration and goes to the lowest configurationally excited state of a 13-atom cluster with a short-range interaction. With this displacement, 12 atoms occupy the same positions as in the ground state, the icosahedron structure, and one atom moves along the higher-energy region of shallow valleys and ridges created by interactions with other atoms. Thus, the coordinate x of Fig. 1c is at first the arc that joins points *1* and *2* in Fig. 1a, when an atom is transferred between these positions such that the equilibrium interatomic distances remain equal to the bond length R_0 of an atomic pair. This establishes the analogy between the phase transition and a transition between configurational states of this cluster that correspond to local minima of its PES.

This description of the cluster behavior on its PES is appropriate for dielectric clusters. There are many configurational states of a metal cluster accessible with a low configurational excitation, and several atoms may partake in this transition. Therefore, the simple form of interpreting such a behavior in terms of the PES is not productive for metal clusters. It is better to use the electronic spectrum for metal clusters that consists of separate bands in the energy space. If the valence band is not completely filled, so that there are empty levels very close to occupied levels, then the cluster exhibits metallic properties. The highest state occupied by electrons is generally called the 'highest occupied molecular orbital' or HOMO for small clusters, by analogy with the terminology for molecules. At low temperatures, the electron energy levels below the HOMO level are occupied, and the behavior of electrons at the HOMO level determines the cluster properties. This cluster description is more productive than that based on the Fermi surface for electrons, a concept more appropriate for bulk materials.

One important mode of studying clusters and their relation to bulk materials relies on connecting the results of numerical simulations with thermodynamics. Indeed, the dynamic character of cluster evolution includes a lot of information, and extraction of its principal and important part leads to a description in thermodynamic terms. Next, the character of cluster evolution depends on external conditions. Figure 2 presents the most common cases of cluster interaction with its environment, when a cluster as a system of atoms is a member of a microcanonical or canonical ensemble. In terms of a Maxwellian ensemble, rather than a Gibbsian ensemble, a single isolated cluster in a vacuum represents a microcanonical ensemble of atoms, whereas a cluster located in a thermostat composes a canonical ensemble of atoms. In

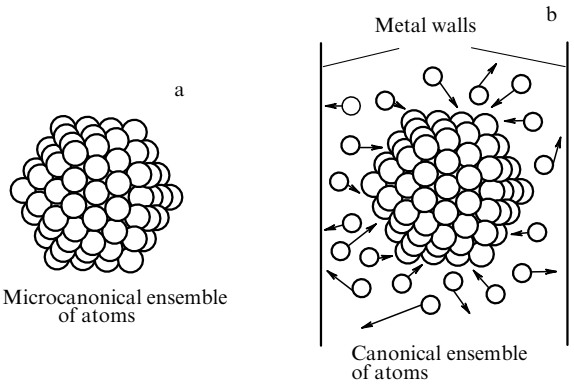

Figure 2. Interaction of a cluster with its environment when the cluster constitutes a microcanonical (a) or canonical (b) ensemble, i.e., is characterized by constant energy or constant temperature, respectively.

experiment, the latter case may be realized if a cluster is placed inside a chamber that is filled with helium (Fig. 2b). Collisions of helium atoms with the chamber walls and with the cluster establishes the cluster temperature equal to the chamber temperature. Experiment and theory reveal that clusters have at least two aggregate states. We will base the following discussion on the supposition that we can deal with just two cluster aggregate states, solid and liquid.

Let us analyze dynamics of the evolution of a cluster with two aggregate states when the following hierarchy of times takes place:

$$\tau \ll \tau_{\mathrm{agg}}\,, \tag{2.2}$$

where τ_{agg} is a typical dwell time for a cluster in each aggregate state, and τ is a typical time between atomic collisions inside the cluster, i.e., a typical time for the establishment of thermal equilibrium of the vibrations. This distinction allows us to introduce the vibrational temperature of the cluster atoms, when this cluster resides in a given aggregate configurational state. Note that this description is independent of the nature of the excited configurational state, i.e., criterion (2.2) relates simultaneously to both dielectric and metal clusters.

We now consider external conditions that affect this cluster. If the cluster is isolated (i.e., it is assumed to be in a microcanonical ensemble and its energy is conserved in time), thermodynamic equilibrium is established during cluster residence in each aggregate state according to criterion (2.2). Therefore, the cluster's state is described by two vibrational temperatures, T_{sol} and T_{liq}, which correspond to the solid and liquid aggregate states. According to the kinetic definition of the temperature, these temperatures are expressed through total kinetic energy K of cluster atoms, averaged during a time that exceeds the period of cluster vibrations. This relationship has the form

$$K = \frac{3n-6}{2}\,T,$$

where n is the number of cluster atoms, and $3n-6$ is the number of vibrational degrees of freedom for this cluster. In the case of the 13-atom cluster, we obtain

$$K_{\mathrm{sol}} = \frac{33}{2}\,T_{\mathrm{sol}}\,, \quad K_{\mathrm{liq}} = \frac{33}{2}\,T_{\mathrm{liq}}\,. \tag{2.3}$$

The other case of external conditions under consideration has to do with the cluster in a thermostat, so that the temperatures T of atoms in both aggregate states are identical, but the total cluster energy is different for the two aggregate states. Of course, in the constant-energy case with the cluster representing a microcanonical ensemble, one can introduce one average temperature T that is expressed through the average kinetic energy of cluster atoms and is averaged over the time during which the cluster undergoes many transitions between aggregate states. Evidently, this temperature is defined as

$$T = w_{\mathrm{sol}}T_{\mathrm{sol}} + w_{\mathrm{liq}}T_{\mathrm{liq}}\,. \tag{2.4}$$

Here, w_{sol}, w_{liq} are the probabilities of the cluster occurrence in the solid and liquid states, respectively.

In considering the behavior of an isolated dielectric cluster and characterizing it by one PES, we find for the total energy of cluster atoms:

$$E = U + K\,, \tag{2.5}$$

where K is the total kinetic energy of atoms, and U is the internal potential energy of the cluster that corresponds to the cluster's location near a particular local minimum of the PES. Let us introduce the cluster aggregate states, including to each of them the regions in the vicinity of local minima of the PES with similar energies. Hence, we define the cluster aggregate state as a set of states with similar potential energies [50 – 52], i.e., they relate to corresponding local minima of the PES.

Thus, restricting our discussion to two aggregate states, we find the total energy of cluster atoms for the solid (E_{sol}) and liquid (E_{liq}) aggregate states in the form

$$E_{\mathrm{sol}} = E_0 + K_{\mathrm{sol}} + U_{\mathrm{sol}}\,, \quad E_{\mathrm{liq}} = E_0 + \Delta E + K_{\mathrm{liq}} + U_{\mathrm{liq}}, \tag{2.6}$$

where E_0 is the total energy of atoms in the solid state at zero temperature, ΔE is the energy of configurational excitation to reach the liquid state, K_{sol} and K_{liq} are the total atomic kinetic energies for the solid and liquid aggregate states, respectively, and U_{sol} and U_{liq} are the total atomic potential energies relating to those of the optimal atomic configuration, the global energy minimum.

We now construct the cluster thermodynamic model in a range of phase coexistence for two cluster aggregate states [50 – 52], and on the basis of this model we transfer from a dynamic cluster description to a thermodynamic one. Separating thermal and configurational degrees of freedom [33], we assume that the atomic thermal vibrational motion of atoms in the vicinity of a chosen local minimum of a PES is a sum of classical cluster oscillations, and that thermodynamic equilibrium is established among the vibrational modes corresponding to criterion (2.2). Then it is possible to construct a strict thermodynamic theory [53] for each aggregate state; it is especially easy if we accept these vibrations as harmonic.

In reality, it is necessary for several reasons to take into account anharmonicity in cluster oscillations, describing it by the anharmonicity parameter η — the ratio of the total kinetic energy K of the atoms in this aggregate state to the total excitation energy $U + K$ for this state. For a purely harmonic system, this parameter of course has the value of $1/2$. Note that a cluster as a system of a finite number of atoms is characterized by large fluctuations due to cluster oscillations, while our present treatment ignores these fluctuations. There-

fore, the quantities under consideration are averaged in time, and a typical average time significantly exceeds a typical period of cluster oscillations.

Thus, with these assumptions, we can transfer from a dynamic description of clusters as atomic systems to their thermodynamic description, thus dealing with average values of energies; the anharmonicity parameter is then introduced as

$$\eta_{\rm sol} = \frac{K_{\rm sol}}{K_{\rm sol} + U_{\rm sol}}\,, \quad \eta_{\rm liq} = \frac{K_{\rm liq}}{K_{\rm liq} + U_{\rm liq}}\,. \tag{2.7}$$

Because the liquid configuration of atoms is looser, $\eta_{\rm liq} < \eta_{\rm sol}$ at any temperature where both aggregate states are present. In the case of harmonic cluster oscillations, $\eta = 1/2$, and formula (2.6) takes the form

$$E_{\rm sol} = E_0 + \frac{3n-6}{2}\,T_{\rm sol}\,, \quad E_{\rm liq} = E_0 + \Delta E + \frac{3n-6}{2}\,T_{\rm liq}\,, \tag{2.8}$$

where n is the number of cluster atoms. In reality, the anharmonicity coefficient is close to 1/2, but its difference from one-half significantly influences cluster properties.

Note that equilibrium between two aggregate states of a dielectric cluster, which determines phase coexistence, is expressed through the entropy jump in the phase transition, i.e., the difference in entropies for the states participating in transitions. For a macroscopic atomic system, the temperature dependence for the entropy jump is not essential because the temperature range for the phase transition is extremely narrow, but for clusters this dependence may be important. The entropy jump is summed from two parts, due to configurational excitation and to atomic vibrations in the cluster. The first part is independent of the temperature, while the second part is zero for harmonic atom vibrations. Therefore, the anharmonicity determines the entropy part that is connected with thermal atomic motion. Then the looser liquid state is characterized by a lower value of the anharmonicity parameter. Since the contribution of atomic thermal motion to the entropy jump is significant, the deviation from 1/2 of the anharmonicity parameter η that is defined by formula (2.7) is significant both for the value of the entropy jump that determines the melting point and for the temperature dependence of the entropy jump that is responsible for the character of phase coexistence.

3. Melting of a 13-atom cluster

3.1 Aggregate states of the 13-atom Lennard-Jones clusters

A cluster consisting of 13 atoms is a convenient system for studying cluster properties. This cluster has an icosahedral structure with a filled atomic shell in the ground state, virtually independent of the interaction between atoms. A large energy gap separates this state from the lowest configurationally excited state and allows one to extract the configurational excitation for a 13-atom cluster in a very straightforward way, as we have seen. Next, its small number of atoms makes this system convenient for computer simulation; yet, simultaneously, this cluster contains enough atoms to model some its properties within the framework of classical thermodynamics. Interactions of atoms in the course of their motion establish statistical equilibrium among cluster oscillations and allow one to describe the thermal motion of atoms by a certain temperature. The statistical distribution of atoms, at least for the ground state with the icosahedral cluster structure, is established faster than transitions involving a change of atomic configuration. This allows one to analyze the role of configurational excitation in the phase transitions of a 13-atom cluster in the optimal way.

We start from the 13-atom Lennard-Jones cluster (i.e., with the Lennard-Jones interaction between cluster atoms) or a cluster with a pair interaction of atoms for which a short-range interaction dominates. Then it is simple to construct the lowest configurationally excited state of this cluster as a result of the formation of a perturbed vacancy in the atomic shell, as shown in Fig. 1a. For formation from the ground configurational state (the solid aggregate state) of this lowest configurationally excited state (the liquid aggregate state) within the framework of our model it is necessary to transfer one atom from the cluster shell to the cluster surface in such a way that it is not contiguous with the newly formed vacancy. After this, atoms shift slightly as a result of their interaction, and the newly formed atomic configuration will correspond to the lowest excited configurational state.

It should be noted that the principal cluster property of phase coexistence in clusters near melting point was discovered for just the 13-atom Lennard-Jones cluster [19 – 25, 27, 28]. The historical basis for the analysis of phase coexistence was computer simulation of this cluster, primarily by the method of molecular dynamics (but also by the Monte Carlo method), and thermodynamic cluster parameters can be inferred from the results of such cluster simulations.

The evolution of a cluster in an excited aggregate state corresponds mainly to the motion of the promoted atom over the cluster surface and to the exchange of the promoted atom with shell atoms. This latter process proceeds more effectively than the process of atomic motion within the icosahedral shell with the vacancy. Therefore, the configurational excitation in Fig. 1a may be considered as representing the liquid aggregate state. As seen from Fig. 1a, c, the lowest configurational excitation of a 13-atom cluster includes only one elementary excitation. Though not all configurational excitations are equivalent, it is attractive to use the model that considers configurational excitation of a dielectric cluster as a sum of elementary configurational excitations, with these excitations being distinguished from thermal excitations. This separation of the degrees of freedom allows one to understand the nature of configurational excitation for a 13-atom cluster and, from that, for larger clusters. If the atomic interaction comprises a long-range component, but interaction between nearest neighboring atoms dominates, the character of configurational excitation is identical for various interaction potentials of atoms, as shown in Fig. 1 for a 13-atom cluster.

The dynamics of cluster evolution may be considered in terms of the potential energy surface of the system in a many-dimensional space of atomic coordinates [48, 49, 54]. This approach is convenient for clusters with short-range interaction, for which interaction between nearest neighbors dominates. If a long-range interaction is also present, we cannot use as the energy of configuration excitation $3D$ and as the barrier height D in the case of a short-range interaction (D is the energy needed to break one bond), although the general character of configurational excitation is conserved. Figure 3 [55] displays excited cluster configurations, the energies of excitation for these configurations, and the energies of saddle points for the 13-atom Lennard-Jones cluster. Comparison of these values with those in the case of a short-range atomic

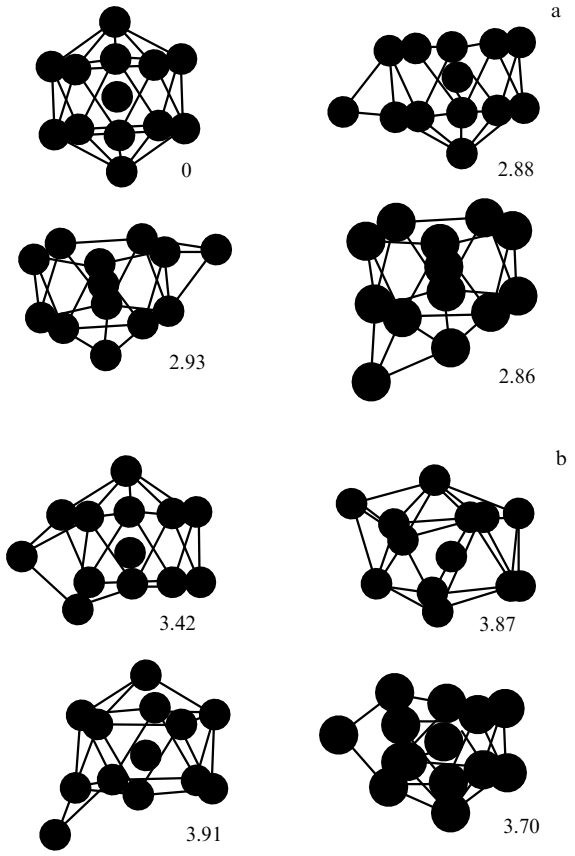

Figure 3. Atomic configurations for (a) excited cluster states and (b) saddle points for the 13-atom Lennard-Jones cluster [55]. Numbers indicate the excitation energy for a given atomic configuration in units of D, the energy needed to break one bond between two atoms.

interaction shows the identical character of excitation in these examples but different values of the parameters which are responsible for this excitation.

We now examine the coexistence of phases in the Lennard-Jones cluster when a cluster is found in the solid aggregate state part of the time, and the rest of the time it resides in the liquid aggregate state. Ignoring fluctuations, we see that the total kinetic energy or the total potential energy of cluster atoms will vary in time as shown in Fig. 4a, which corresponds to the validity of criterion (2.2). In reality, fluctuations are of course present, as we can see in Figs 4b and 4c, also based on computer simulations [56, 59]. Nevertheless, the latter dependences may be approximated by the dependence plotted in Fig. 4a.

The 13-atom Lennard-Jones cluster was studied by MD computer simulation in both ensembles, canonical [54] and microcanonical [23]. We next use the results of these studies to examine cluster behavior in the range of phase coexistence. The existence of two aggregate cluster states follows from Fig. 5 which gives the distributions of potential energies for the 13-atom Lennard-Jones cluster under isothermal conditions at various temperatures, with the maxima of this distribution relating to the two aggregate cluster states. The bimodal forms of these distributions testify to the existence of two aggregate states in the coexistence range. A general characteristic of behavior in the range of phase coexistence is that the liquid state is 'looser' and is therefore characterized by parameters with stronger temperature dependence than those of the solid state. Therefore, the anharmonicity

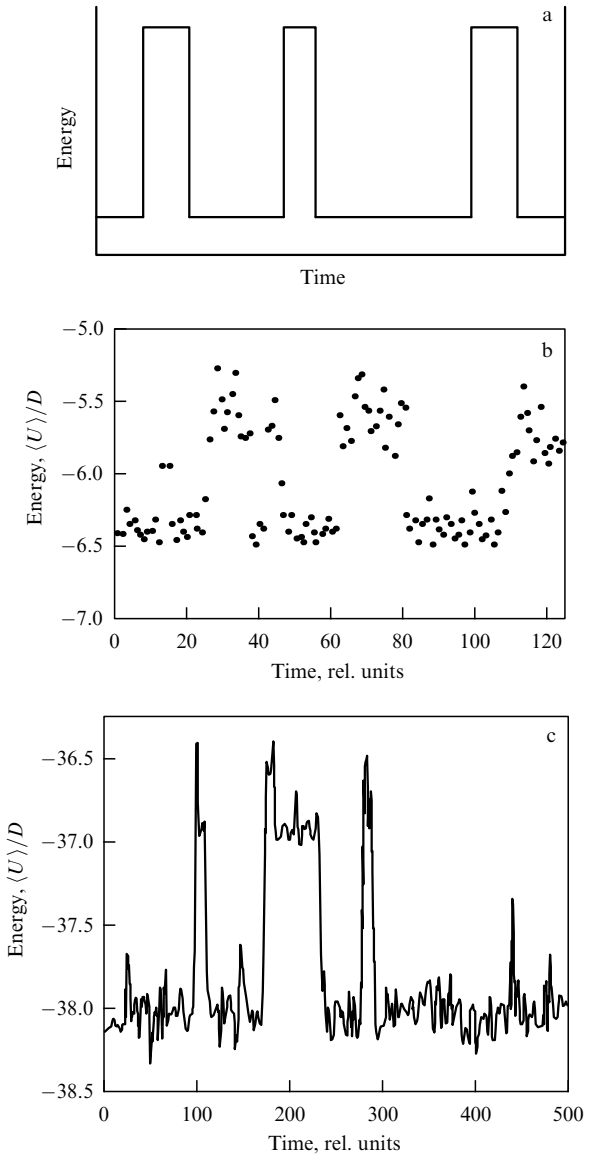

Figure 4. Time variation of the total potential energy of cluster atoms: (a) averaged over all the fluctuations, the total potential energy in a range of phase coexistence; (b) averaged over cluster oscillations, the total potential energy of cluster atoms for the isothermal 13-atom Lennard-Jones cluster according to computer simulation [56], and (c) the same quantity for the isolated 13-atom Lennard-Jones cluster at the excitation energy of $10.8D$, below the melting energy ($13.8D$) according to computer simulation [59].

parameter and the contribution of thermal motion of atoms to the entropy jump in the phase transition is determined by the liquid aggregate state.

For the 13-atom Lennard-Jones cluster at constant energy [23] we can extract the energy ΔE of configurational excitation and the anharmonicity parameters $\eta_{\rm sol}$ and $\eta_{\rm liq}$ from computer simulation data for the solid and liquid cluster states in the range of phase coexistence. It should be emphasized that in formulas (2.3) the temperatures of the solid ($T_{\rm sol}$) and liquid ($T_{\rm liq}$) aggregate states are expressed in terms of the mean kinetic energies of atoms for the solid ($K_{\rm sol}$) and liquid ($K_{\rm liq}$) aggregate states at each energy of cluster excitation, $E_{\rm ex} = E - E_0$. The treatment of data [23] from computer simulations of the Lennard-Jones cluster reveals that the energy ΔE of the phase transition is effectively

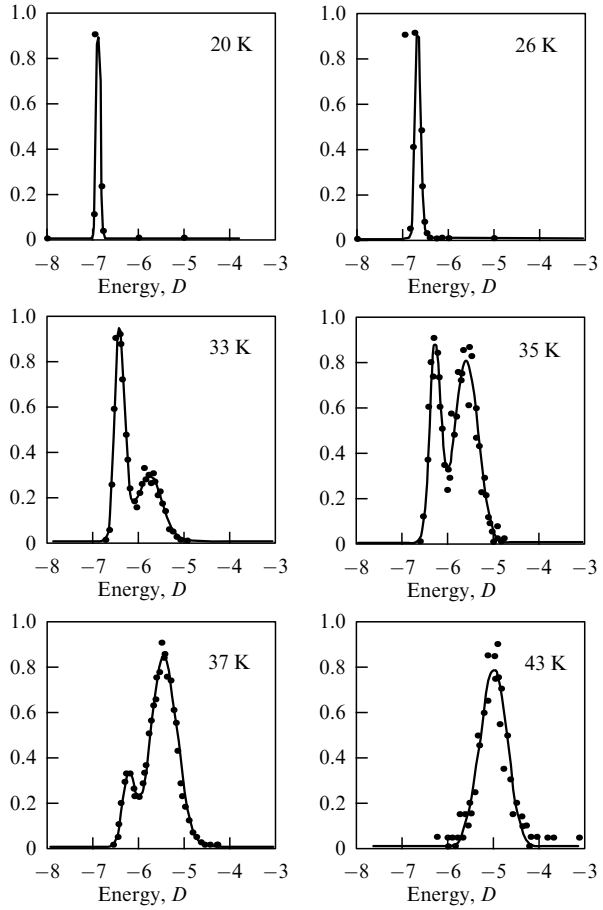

Figure 5. The distribution of the total potential energies of cluster atoms for the isothermal 13-atom Lennard-Jones cluster [56]. The potential energy is averaged over times which exceed cluster oscillation periods and are less than the time required for the system to explore more than one of the regions around a single local minimum configuration. The energy is expressed in units of D, the bond dissociation energy.

independent of the total cluster energy in the range of phase coexistence and is given by [32, 57, 58]

$$\Delta E = (2.40 \pm 0.05)\, D\,. \tag{3.1}$$

The anharmonicity parameters defined for the solid and liquid aggregate states of the isolated 13-atom Lennard-Jones cluster according to formulas (2.7) are presented in Fig. 6 [29, 32] as the functions of temperature. These dependences result from a treatment of the data from computer simulation [23]; they may be utilized whether the cluster constitutes a microcanonical or canonical ensemble of atoms and are reduced to the temperatures of the corresponding aggregate states. Note that the anharmonicity parameter η defined according to formulas (2.7) takes essentially identical values for this Lennard-Jones cluster under adiabatic conditions for the solid and liquid aggregate states at their temperatures, $\eta_{\rm sol}(T_{\rm sol}) = \eta_{\rm liq}(T_{\rm liq})$, within the limits of accuracy for these quantities. This confirms the fact that the anharmonicity of vibrations for a looser liquid state shows up at lower temperatures than that for the solid state. In addition, Table 1 contains some parameters of the 13-atom Lennard-Jones cluster. It should be noted that the temperature dependence for the anharmonicity parameter of the liquid state, given in Fig. 6, is derived from computer simulation for this cluster [56], treated as a canonical ensemble of atoms.

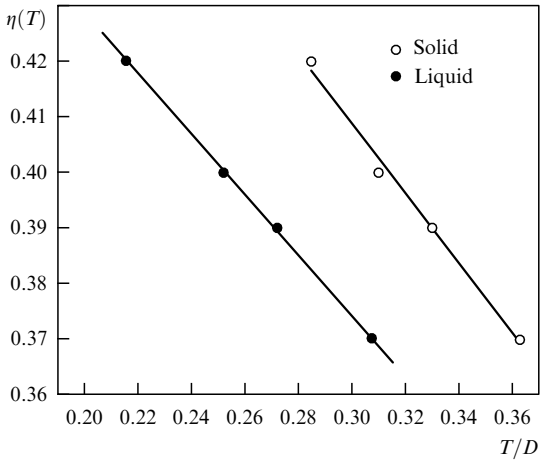

Figure 6. The anharmonicity parameters for the solid and liquid aggregate states of an isolated 13-atom Lennard-Jones cluster as functions of the effective cluster temperature [29, 32] based on the mean kinetic energy, which follow from data of computer simulation [23].

Table 1. Parameters of an isolated 13-atom Lennard-Jones cluster under constant-energy conditions, which follow from computer simulation [23]; the energies and temperatures are expressed in units of dissociation energy D per one bond.

$E_{\rm ex}/D$	11	12.9	14.1	16.2
$K_{\rm sol}/D$	4.63	5.11	5.44	6.00
$K_{\rm liq}/D$	3.56	4.15	4.48	5.07
$T_{\rm sol}/D$	0.285	0.310	0.330	0.363
$T_{\rm liq}/D$	0.216	0.252	0.272	0.307
η	0.42	0.40	0.39	0.37
p	0.1	0.4	1.8	4.0
$\Delta E/D$	2.5	2.4	2.5	2.5
$\Delta T/D$	0.059	0.058	0.058	0.056
$\Delta S(T_{\rm liq})$	6.9 ± 0.4	7.5 ± 0.4	8.5 ± 0.3	8.6 ± 0.3

Defining the melting temperature $T_{\rm m}$ of an isothermal cluster in the following form

$$T_{\rm m} = \frac{\Delta E}{\Delta S}\,,$$

taking the above value of the energy jump ΔE as characteristic of the phase transition for the 13-atom Lennard-Jones cluster, and ignoring the deviation of the temperature dependence of the entropy jump from that at zero temperature, $\Delta S = \ln 180 = 5.2$, we obtain for the melting point: $T_{\rm m} \approx 0.5D$. When we employ the data of Table 1 to account for the temperature dependence of the cluster parameters, we obtain an entropy jump at the melting point $\Delta S \approx 8$ and the melting point $T_{\rm m} \approx 0.3D$. From this we see the importance of the temperature dependence of cluster parameters in the range of phase coexistence for the character of the phase transition. Note that if a cluster could be modelled as a sum of harmonic oscillators in both the solid and liquid states, the temperature dependence for cluster parameters would be weak. Therefore, an important set of quantities that characterizes the behavior of a cluster in the range of phase coexistence are the anharmonicity parameters $\eta_{\rm sol}$ and $\eta_{\rm liq}$.

We add to the thermodynamic parameters of the isolated 13-atom Lennard-Jones cluster information that follows from computer simulation when this cluster constitutes a canonical ensemble of atoms [56] and the phase transition energy is given by formula (3.1). On the basis of the results of

computer simulation one can construct caloric curves for the solid $[E_{\rm sol}(T)]$ and liquid $[E_{\rm liq}(T)]$ aggregate states, and the difference between these quantities is given by the formula

$$E_{\rm liq} - E_{\rm sol} = \Delta E + \frac{33}{2}\, T\left[\frac{1}{\eta_{\rm liq}(T)} - \frac{1}{\eta_{\rm sol}(T)}\right]. \qquad (3.2)$$

Because under isothermal conditions the relationship $T_{\rm sol} = T_{\rm liq} = T$ is true, we have $\eta_{\rm sol}(T) > \eta_{\rm liq}(T)$, and the above energy difference between the two phases exceeds the energy of configurational excitation [32] determined by formula (3.1) for an isolated cluster. Figure 6 depicts the temperature dependences of the anharmonicity parameters $\eta_{\rm sol}$ and $\eta_{\rm liq}$ in a range of phase coexistence and allows us to determine the difference between these energies $E_{\rm liq}(T)$ and $E_{\rm sol}(T)$ on the basis of results obtained from computer simulation of the isolated, constant-energy 13-atom Lennard-Jones cluster [23]. The analysis of this computer simulation also shows that the anharmonicity parameters for the solid and liquid states are identical for the isolated 13-atom Lennard-Jones cluster, whereas the temperature of the liquid state is lower than that for the solid state.

Figure 7 presents the analog of caloric curves for the isothermal 13-atom Lennard-Jones cluster — the total potential energies for atoms of this cluster that are obtained from computer simulation [56] of this cluster and computed on a scale such that $U_{\rm sol} = 0$ at $T = 0$. These data allow one to check the model according to which the motion of the atoms is a sum of slightly anharmonic vibrations. In the limit of low temperatures, the heat capacity of this cluster is $C = K/T = 33/2$, in accordance with the definition of the temperature for both aggregate states, where K is the total kinetic energy of cluster atoms. The anharmonic model we are using gives the following expressions for the potential energies of the solid ($V_{\rm sol}$) and liquid ($V_{\rm liq}$) aggregate states:

$$V_{\rm sol} = C\left[\frac{1}{\eta_{\rm sol}(T)} - 1\right], \quad V_{\rm liq} = \Delta E + C\left[\frac{1}{\eta_{\rm liq}(T)} - 1\right]. \qquad (3.3)$$

Figure 8 demonstrates the temperature dependences of the parameters

$$\xi_{\rm sol} = \frac{U_{\rm sol}(T)}{V_{\rm sol}(T)}, \quad \xi_{\rm liq} = \frac{U_{\rm liq}(T) - \Delta E}{V_{\rm liq}(T) - \Delta E}. \qquad (3.4)$$

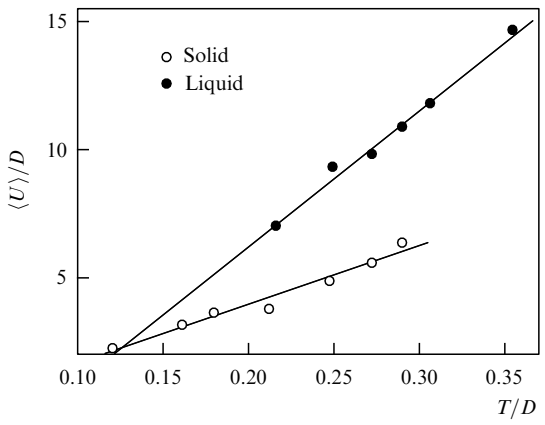

Figure 7. The total potential energy of atoms for the isothermal 13-atom Lennard-Jones cluster relating to the global energy minimum for this cluster at $T = 0$ and averaged over cluster oscillations.

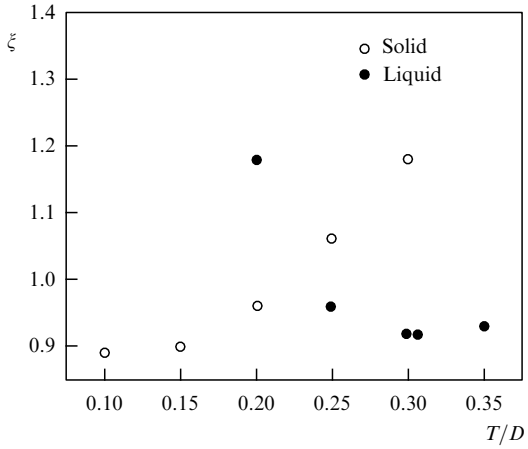

Figure 8. The ratio (3.4) of the total potential energy of cluster atoms to that described by formula (3.3) for an anharmonic model applied to the 13-atom Lennard-Jones cluster.

These parameters would be equal to unity for the model of harmonic oscillators. As follows from Fig. 8, the model of slightly anharmonic oscillators holds true more or less for the solid aggregate state, while it describes the liquid aggregate state significantly less well. The reason for this behavior is that an atom located on the cluster surface executes a free motion over that surface rather than just a small-amplitude vibrational motion.

This information about the 13-atom Lennard-Jones cluster is enriched by the data describing the character of equilibrium between aggregate states at a given temperature. Let us introduce the equilibrium constant p in the following way:

$$p = \frac{w_{\rm liq}}{w_{\rm sol}}, \qquad (3.5)$$

where $w_{\rm sol}$ and $w_{\rm liq}$ are the probabilities of a cluster occurrence in the solid and liquid states, respectively, and under these conditions $w_{\rm sol} + w_{\rm liq} = 1$, which gives for these probabilities:

$$w_{\rm sol} = \frac{1}{1+p}, \quad w_{\rm liq} = \frac{p}{1+p}. \qquad (3.6)$$

One can introduce the configurational temperature $T_{\rm con}$ that can differ from the vibrational temperature and is given implicitly by the relationship

$$p = \exp\left(-\frac{\Delta E}{T_{\rm con}} + \Delta S\right), \qquad (3.7)$$

where ΔS is the cluster entropy change associated with the phase transition. It is clear that if the cluster under consideration is in a canonical ensemble, the configurational temperature $T_{\rm con}$ at equilibrium coincides with the vibrational temperature T of the atoms. If the cluster constitutes a microcanonical ensemble of atoms, the vibrational temperatures are different for the solid ($T_{\rm sol}$) and liquid ($T_{\rm liq}$) aggregate states, and their difference for a 13-atom cluster equals

$$\Delta T = \frac{\Delta E}{C} = \frac{2\Delta E}{33}; \qquad (3.8)$$

if we assume that the vibrations behave classically, then the heat capacity of a 13-atom cluster is $C = 33/2$ (we express temperatures in energy units). In particular, for the Lennard-Jones cluster involving 13 atoms this temperature difference amounts to

$$\Delta T \approx 0.06D\,,$$

and D is again the bond dissociation energy. Evidently, the configurational temperature $T_{\rm con}$ lies between those of the solid ($T_{\rm sol}$) and liquid ($T_{\rm liq}$) states. Next, we shall find the configurational temperature in this case.

Let us use the equation of detailed balance for transition between the solid and liquid aggregate states, which holds under equilibrium conditions:

$$w_{\rm sol}v_{\rm sol}(T_{\rm sol}) = w_{\rm liq}v_{\rm liq}(T_{\rm liq})\,, \tag{3.9}$$

where $v_{\rm sol}$ is the rate of solid-to-liquid transitions, and $v_{\rm liq}$ is the rate of liquid-to-solid transitions. These rates are connected by the principle of detailed balance [40, 57, 60 – 62]

$$\frac{v_{\rm sol}(T)}{v_{\rm liq}(T)} = g\exp\left(-\frac{\Delta E}{T}\right) = \exp\left(-\frac{\Delta E}{T} + \Delta S\right), \tag{3.10}$$

where g is the ratio of statistical weights for the liquid and solid aggregate states that is related to the transition entropy as $\Delta S = \ln g$, and ΔE is the energy of configurational excitation for this transition. Accounting for the basic temperature dependence of the rates of transitions between aggregate states and the activation character of these transitions, we find

$$v_{\rm sol}(T) \sim \exp\left(-\frac{\Delta E}{T} - \frac{E_{\rm b}}{T}\right), \quad v_{\rm liq}(T) \sim \exp\left(-\frac{E_{\rm b}}{T}\right), \tag{3.11}$$

where T is the atomic vibrational temperature for the initial aggregate state, ΔE is the energy of cluster configurational excitation, and $E_{\rm b}$ is the energy of the barrier that separates the local minima of the potential energy surface. From this we obtain the following expression for the equilibrium constant of an isolated cluster:

$$p = \frac{w_{\rm liq}}{w_{\rm sol}} = \exp\left[\Delta S - \frac{\Delta E}{T_{\rm sol}} - E_{\rm b}\left(\frac{1}{T_{\rm sol}} - \frac{1}{T_{\rm liq}}\right)\right]. \tag{3.12}$$

Comparing this expression with the definition of the configurational temperature (3.7), we obtain the formula for the latter:

$$T_{\rm con} = \frac{T_{\rm sol}}{1 + (E_{\rm b}/\Delta E)\,(\Delta T/T_{\rm liq})}\,. \tag{3.13}$$

This relation for the isolated 13-atom Lennard-Jones cluster takes the form ($E_{\rm b} = 0.56D$, $\Delta E = 33\Delta T/2\eta$)

$$T_{\rm con} = \frac{T_{\rm sol}}{1 + 0.034D\eta/T_{\rm liq}}\,. \tag{3.14}$$

From this it follows that the configurational temperature of the cluster considered is closer to the solid temperature than to that of the liquid. In particular, at the melting point, $p = 1$, we have [32] $T_{\rm con} = 0.95T_{\rm sol}^{\rm m} = 0.315D$, while $T_{\rm liq}^{\rm m} = 0.82T_{\rm sol}^{\rm m}$ ($T_{\rm sol}^{\rm m} = 0.33D$, $T_{\rm liq}^{\rm m} = 0.27D$, $\eta_{\rm sol}(T_{\rm sol}^{\rm m}) = \eta_{\rm liq}(T_{\rm liq}^{\rm m}) = 0.39$).

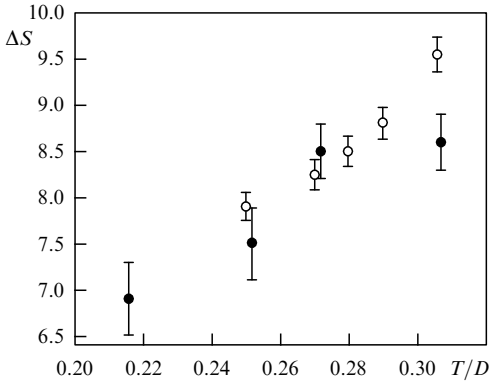

Figure 9. The entropy jump upon melting of the 13-atom Lennard-Jones cluster. Closed circles are obtained from the results of computer simulation of the isolated 13-atom Lennard-Jones cluster [23], and open circles correspond to the isothermal 13-atom Lennard-Jones cluster [56].

On the basis of formula (3.12) for the solid – liquid equilibrium constant p and the values of the latter recovered from computer simulation, one can determine the entropy jump ΔS as a function of temperature in the range of phase coexistence. One can relate the entropy jump to the liquid temperature $T_{\rm liq}$ in a constant-energy computer simulation [23], if we later reduce the entropy jump to the isothermal conditions of the phase transition for the case of the isothermal cluster, given in Table 1 and Fig. 9. We also present in Fig. 9 the entropy jump upon melting, based on the equilibrium constant when these data have been derived from simulations under isothermal conditions [56]. Then, the equilibrium constant is equal to

$$p(T) = \exp\left[\frac{E_{\rm sol} - E_{\rm liq}}{T_{\rm con}} + \Delta S(T)\right]. \tag{3.15}$$

Here we use the energy of configurational excitation rather than the energy difference $E_{\rm liq} - E_{\rm sol}$ for these aggregate states. These values are different due to the anharmonic character of cluster atom vibrations. The degree of coincidence of the entropy jump reduced to isothermal conditions and obtained on the basis of computer simulations for isolated and isothermal clusters (Fig. 9) testifies to the accuracy of this treatment and thermodynamic description of the cluster.

Computer simulation of 13-atom Lennard-Jones clusters by the molecular dynamics method gives a useful experience in the study of cluster behavior in the range of phase coexistence. Detailed information about cluster evolution follows from the dynamic analysis and is richer than that gained from direct application of thermodynamics, but thermodynamical approach reduces the description of cluster behavior to simple and standard schemes on the basis on a restricted number of parameters. In this way we learn that a thermodynamic description of clusters in the range of phase coexistence from the results of dynamic simulation allows one to represent the character of phase coexistence in a simple form.

Side by side with this, the transition from the dynamic cluster description to the thermodynamic one allows us to elaborate simple models for the description of cluster behavior in the range of phase coexistence. Experience in the analysis of the 13-atom Lennard-Jones clusters associ-

ates these peculiarities in the behavior with a small anharmonicity of atomic vibrations in clusters. Introduction of the anharmonicity parameter in the model of phase coexistence exhibits a very significant contribution of thermal atomic motion to the entropy jump in the phase transition, and this contribution increases with increasing cluster temperature.

3.2 Phase transitions in 13-atom metal clusters

One can expect that the analysis of metal clusters is more complicated than that of dielectric ones because of additional degrees of freedom in metal clusters, arising from accessible transitions of electrons. But if the cluster temperature is sufficiently low, electrons occupy the lowest part of their spectral band, so that the cluster's behavior will be determined just by the PES on which the electrons are not excited. Then if the PESs for dielectric and metal clusters are essentially identical, one can expect the same behavior for dielectric and metal clusters. This analogy does hold for 13-atom clusters — the ground configurational states of these clusters, both dielectric and metal, are icosahedral. Nevertheless, a significant difference between these two types of clusters arises from the small energy of configurational excitation and the consequent large number of configurationally excited states for metal clusters, as illustrated in Fig. 10b. This difference becomes apparent in the study of metal clusters. In contrast to Lennard-Jones clusters, for which each aggregate state can be studied separately in the range of phase coexistence, averaging over aggregate states is usual in the study of metal clusters. Even 13-atom metal clusters have large numbers of low-lying configurationally excited states, a property that distinguishes them sharply from dielectric clusters, and this justifies averaging over cluster configurational states in computer simulation. The configurationally excited states of the latter are sparse and well separated in energy for the ground configurational state of the icosahedral structure, and this allows one, in principle, to study separately the ground configurational state that is of importance for information about cluster aggregate states and transitions between them.

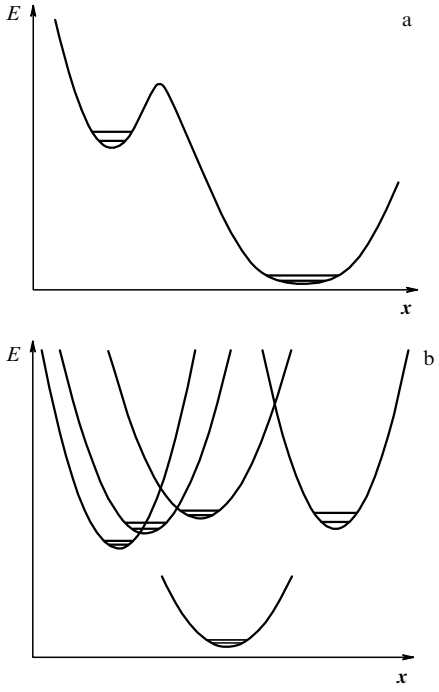

Figure 10. The character of cluster configurational excitation for a cluster consisting of (a) inert gas atoms with one PES, and (b) a metal cluster with many intersecting PESs. The schematic coordinate is chosen in a multidimensional space of atomic coordinates.

To simulate metal clusters reliably, it is necessary to take into account the effects of electron–electron interaction, including exchange interaction and the effects of Fermi–Dirac statistics. Furthermore, the results obtained from any given model must be checked against real data for a macroscopic metal whose measured parameters allow one to correct parameters of the interaction potential for any given configuration of cluster atoms. Such an interaction potential may be used for the analysis of various cluster properties. We list below some papers on 13-atom metal clusters which were studied in this manner: Au [63–71], Mo [72, 73], Pt [74, 75], Al [76–78], Ni [79], Rh [80], Ni, Ag, Au [81], Pd [82], Al, Ni, Cu, Ag, Pd, Pt, Au, Pb [83, 84], Nb [85], Cu, Ag, Au [86, 87], Y, Zr, Nb, Mo, Ru, Rh, Pd, Ag, Cd [88], and Ni, Ag, Au [89]. This list is not exhaustive; it is introduced here as evidence of a wide front of studies for 13-atom metal clusters.

It should be noted that 13 is the magic number both for clusters of noble metals and for more reactive metals, such as Fe, Ti, Zr, Nb, Ta [90], and the icosahedral structure corresponds to the PES global minimum in practically all the 13-atom metal clusters. This was called into question for 13-atom gold clusters with the relatively lowest energy of configurational excitation. Indeed, according to Refs [63–65, 67, 68], the icosahedral structure corresponds to the global energy minimum, although, according to Refs [63, 69, 86], the icosahedral structure is appropriate to the lowest configurationally excited state. Thus, the sequence of configurational levels inferred from simulations depends on the choice of atomic interaction model for the computer simulation. In any case, the energy gap between the ground and lowest excited configurational states in gold is relatively small, and relativistic effects are strong in their influence on hybridization of the s and d shells of the atomic valence electrons. This causes mixing of cluster structures even at low temperatures. Along with cuboctahedral and decahedral structures, amorphous and planar atom distributions can partake in structure mixing, though no simulation has yet been done with a strongly correlated basis for the electrons.

If the energy gap between the ground and lowest configurationally excited states is small, the question arises about the absence of the phase transitions for gold and other metal clusters with electron coupling neglected. Indeed, if the cluster excitation energy is low and the spectrum of configurational excitations is almost continuous, it is problematic to separate energetically the cluster aggregate states if these are composed of configurational states of the cluster. We cannot answer this question in the simple terms which are used for dielectric clusters, but one can rely on the results that in all cases of experimental studies or computer simulations there are both solid and liquid aggregate states. Although the solid and liquid phases are not separated in computer simulations of metal 13-atom clusters, these clusters have two different aggregate states. This follows, in particular, from the temperature dependences of the heat capacities of the clusters, which are characterized by their peaked, resonant shape, as is well known for traditional phase transitions. Nonetheless, it seems plausible that the existence of those two observable aggregate states in metal clusters is connected with the behavior of the electron component.

We next consider certain simulations of metal clusters and the results of such simulations that give us an insight into the properties of metal clusters. The interaction potential in metal clusters is of course more complicated than that used in describing the dielectric system. In addition to accounting for the interaction between atomic cores, the effective potential must include electron coupling. Nevertheless, this can be taken into consideration in a simple way in some models that conserve the pair form of the interaction potential. Indeed, separating the interaction potential between cores and the electron coupling, one can represent the interaction potential in the form [91]

$$U = \sum_{i,k} V(r_{ik}) - a \sum_{i} \sqrt{N_e}\,, \tag{3.16}$$

where r_{ik} is the distance between nuclei i and k, $V(r)$ is the interaction potential between two atomic cores at separation r between them, a is a numerical coefficient, and N_e is the electron number density. The first term of this formula corresponds to repulsion between atomic cores and has the form $V(r) \sim r^{-n}$, where n is the appropriate factor. Electron coupling described by the second term in formula (3.16) depends on the electron density in atomic cores because electrons are attached to cores. Then, one form of the potential energy, the Sutton – Chen interaction potential, is given by [92]

$$U = D\left[\sum_{i \neq k} \left(\frac{R_e}{r_{ik}}\right)^n - C \sum_{i \neq k} \left(\frac{R_e}{r_{ik}}\right)^m\right]. \tag{3.17}$$

Thus, in spite of the different character of interaction in metal and dielectric clusters, one can, at least to some degree of approximation, reduce the potential energy of atoms in metal clusters to a form similar to that of Lennard-Jones clusters. The parameters of this potential may be determined in its application to bulk metals. In this operation we assume that a metal cluster is an element that is cut from bulk metal, taking into account surface effects.

We have ascertained that the potential energy surface of a cluster of metal atoms may be similar to that of a cluster of dielectric atoms or of weakly interacting atoms for which a pairwise form of the potential energy is valid. Note that the Sutton – Chen form (3.17) of the potential energy is empirical, and its parameters must be inferred from the properties of real metals. Of course, different forms of potential energies are also used for treating the properties of small metal clusters (see, for example, Refs [75, 93 – 98]). The most appropriate form may depend on what metal we are examining. Table 2 contains parameters of the Sutton – Chen interaction potential for some metals [89, 99] we consider below; these parameters follow from the constraint that the parameters of bulk metals must be described by this interaction potential.

The Sutton – Chen form of potential naturally presents metal clusters as similar, structurally, to Lennard-Jones clusters. Based on the results of numerical simulations [70, 71, 89], we give some results for 13-atom metal clusters in analogy with the Lennard-Jones cluster. Comparing the two kinds of systems gives us insight into the origin of the values of the parameters for these clusters, and also of the information content of these models for computer simulation.

Basing our treatment on analogy with dielectric clusters, we consider the phase transition in metal clusters as configurational excitation in accordance with Fig. 1c. Then for 13-atom metal clusters, the global energy minimum corresponds to the icosahedral geometry, and this minimum is

Table 2. Parameters of the interaction potential (3.17) of bulk metals [89, 99].

	n	m	D, meV	C	R_e, Å
Ni	9	6	16	39	3.52
Ag	12	6	2.5	144	4.09
Au	10	8	13	34	4.08

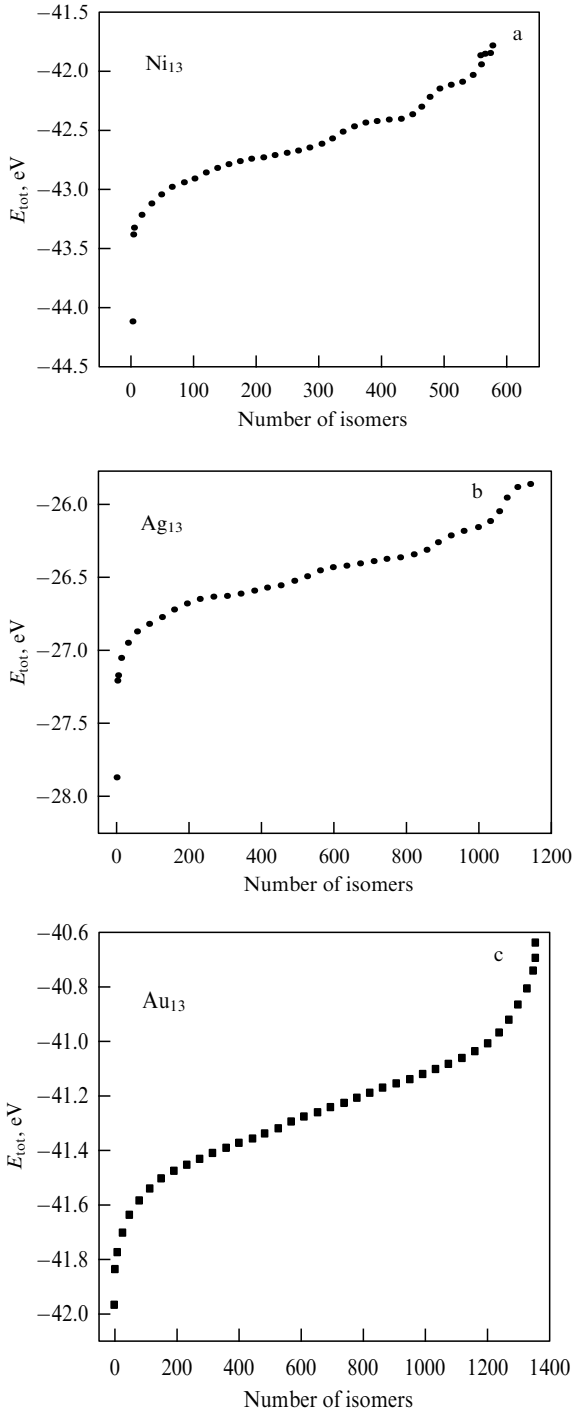

Figure 11. The number of isomers for metal clusters comprising 13 atoms [89].

separated by an energy gap from configurationally excited states whose energies are very close and can effectively be treated as a continuous band in accordance with Fig. 10b. Then, the number of possible configurational states, equivalent to the number of isomers, increases with the excitation energy, as shown in Fig. 11. Hence, the liquid state of metal clusters constitutes a mixture of many atomic configurations whose number grows with increasing excitation energy. Although the properties of these states are determined by the behavior, especially the interactions, of the valence electrons, the liquid state of metal clusters remains analogous to that of Lennard-Jones clusters, at the very least because the melting process involves similar changes of atomic configurations. For this reason, both cluster types exhibit two aggregate states despite the fact that the liquid aggregate state of metal clusters involves another, altogether different kind of interaction.

The indicator of the phase transition for clusters is the change in character of atomic motion, and the appropriate parameter indicating this is the fluctuation of bond length. Naturally, in the liquid state, atoms acquire a higher mobility to move within the cluster, and this parameter increases sharply at melting. Commonly, the relative root mean square of the bond-length fluctuation δ is used as the indicator of this behavior. It is expressed as

$$\delta = \frac{2}{n(n-1)} \sum_{i<j} \left[\frac{\langle r_{ij}^2 \rangle - \langle r_{ij} \rangle^2}{\langle r_{ij}^2 \rangle} \right]^2 , \qquad (3.18)$$

where r_{ij} is the distance between i and j atoms, n is the number of atoms in a cluster, and the angle brackets mean an average over fast atomic vibrations. This approach was first introduced by Lindemann [100], who used atomic fluctuations from equilibrium positions as the measure, but further, slightly more indicative parameters based on interparticle distances have been utilized in Refs [21, 22, 101, 102], and formula (3.18) gives the widespread form of the correlation function [23, 103]. For the solid cluster state, in which atoms are tied closely to lattice sites, parameter (3.18) is typically smaller than 0.1, and it increases sharply at melting. Figure 12 gives the caloric curve for silver clusters consisting of 13 and 14 atoms [89], in which some points are indicated that are of interest for the phase transitions. Figure 13 displays the temperature dependence of the reduced bond-length fluctuation δ defined by formula (3.18) for clusters Ar_{13}, Ag_{13}, and Ag_{14}. One can see that the parameter δ exhibits a jump precisely around the melting point of this cluster. This jump may be used as the basis for definition of the melting point from computer simulations, although the 'jump' clearly takes place over a finite temperature interval. On the basis of the behavior of parameter (3.18), one can conclude that such a phase transition occurs for all sufficiently small metal clusters.

The points marked in Fig. 12 with numbers indicate different ranges of cluster states. In particular, the temperature *1* corresponds to the solid cluster state, *2*, the point of inflection, is the melting point, and *3* lies in the liquid region. In the case of the Ag_{14} cluster, the structure of the parameter δ is more complicated and gives evidence of two-stage melting. In particular, the second jump of δ near point *4* testifies to the appearance of a new group of cluster structures. It is an open question, perhaps a semantic one, as to whether we can consider the regions around *3* and *4* points as indicating two different phases.

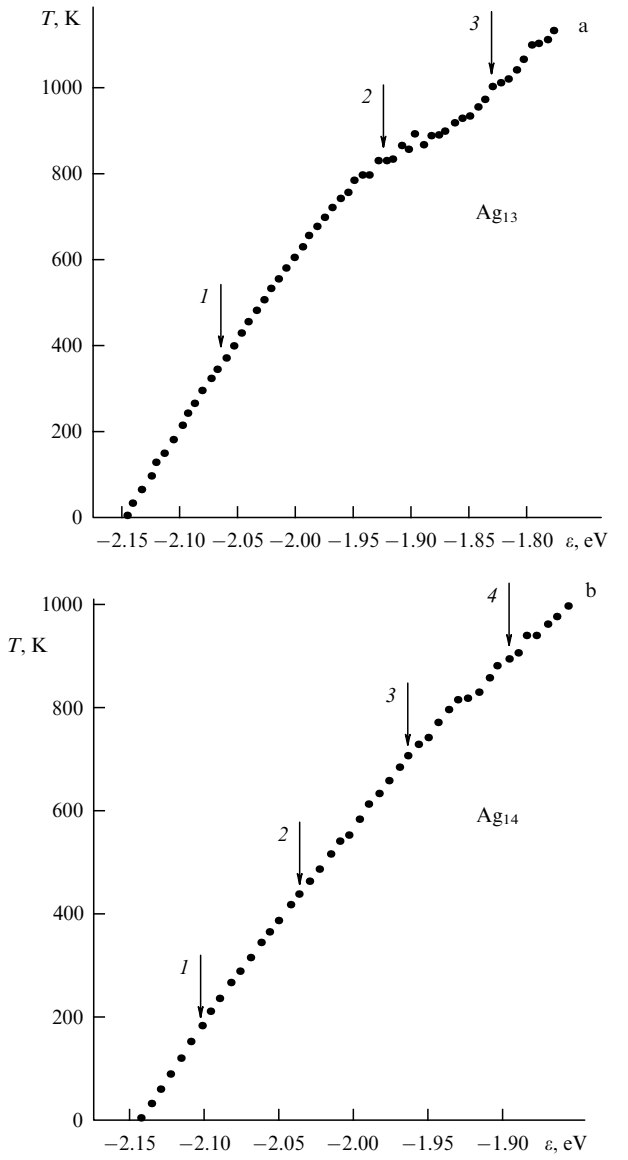

Figure 12. Caloric curves for clusters Ag_{13} (a) and Ag_{14} (b) [89].

Larger clusters, e.g., consisting of 45 or 50 atoms or more, clearly exhibit more than two distinct phases [26, 27]. In any case, the 13-atom clusters which have completed icosahedral shell structures for their ground states are characterized by a simpler kind of melting, as well as by higher melting temperatures than clusters of neighboring sizes with incomplete outer atomic shells. As a demonstration of this fact, Fig. 14 indicates the melting points of Lennard-Jones clusters reduced to the interaction of argon atoms, and the melting points of metal clusters of different sizes according to simulation [89]. We see that the melting point is a nonmonotonic function of cluster size and clusters of magic sizes are characterized by higher melting points than clusters of neighboring sizes.

One notable peculiarity of metal clusters, as compared to dielectric (Lennard-Jones) clusters, is their relatively small fusion energies. From Fig. 12 it follows that metal cluster melting becomes apparent only weakly in the caloric curves because of those small fusion energies. In addition, Table 3 gives the values of the binding energy ε_0 and the fusion energy ΔH_{fus} per atom for bulk argon and some metals. These values

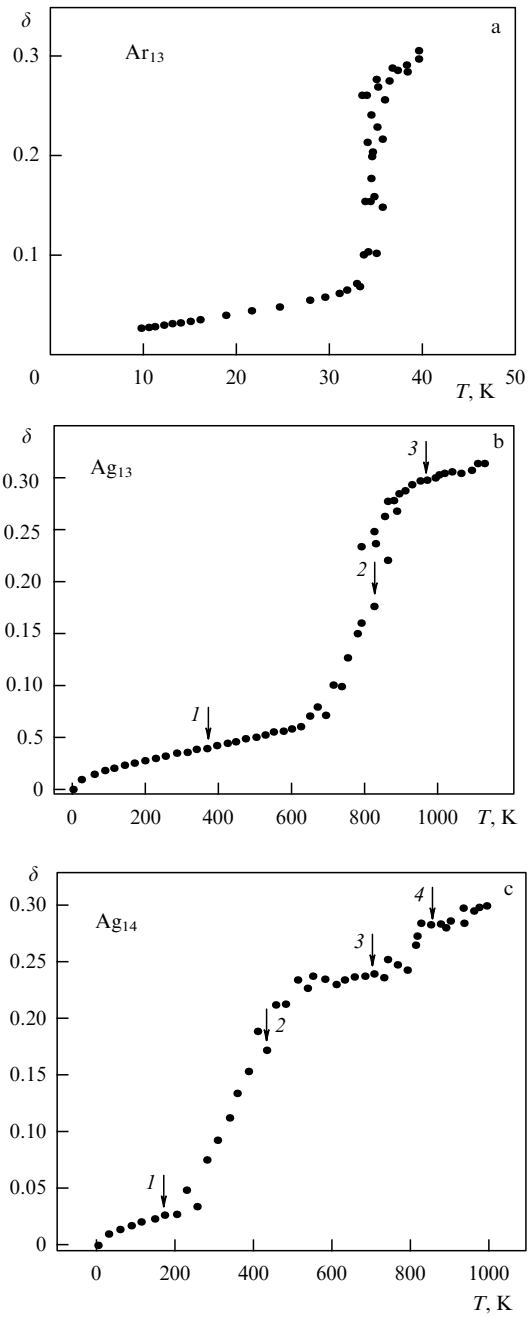

Figure 13. The root mean square δ for fluctuations of cluster bond lengths according to formula (3.18) for the Lennard-Jones cluster Ar_{13} [105] (a), for the cluster Ag_{13} [89] (b), and for the cluster Ag_{14} [89] (c).

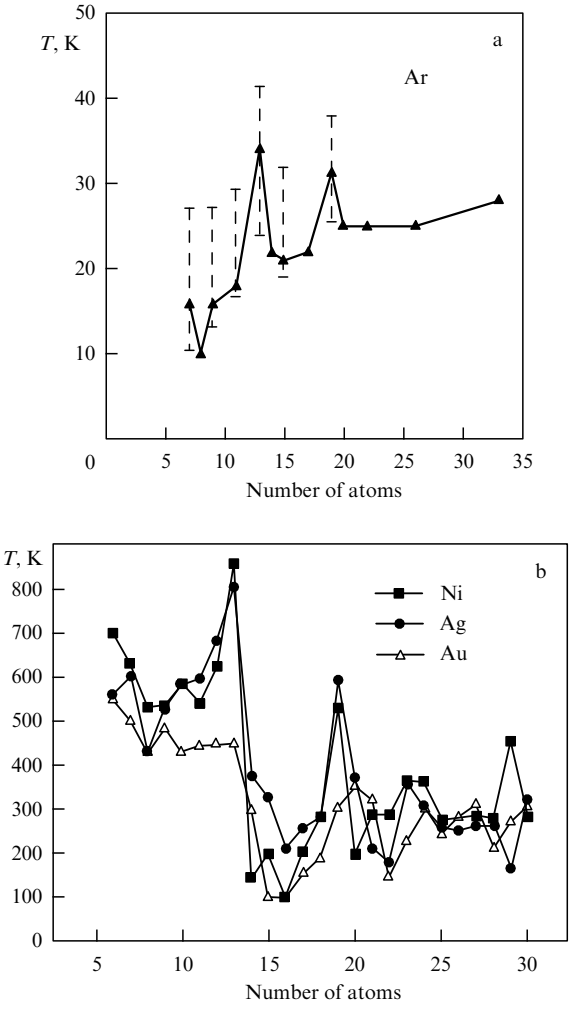

Figure 14. (a) The melting points (triangles) of Lennard-Jones clusters reduced to the interaction of argon atoms of various sizes and a range of phase coexistence [105], and (b) the melting points of nickel, silver, and gold clusters of different sizes [89].

Table 3. Parameters of bulk metals.

Bulk	ε_0, eV	ΔH_{fus}, eV	$\Delta H_{\text{fus}}/\varepsilon_0$, %
Ar	0.068	0.0123	18
Ni	4.13	0.181	4.4
Cu	3.40	0.138	4.1
Ag	2.87	0.120	4.2
Au	3.65	0.130	3.6

confirm the above statement and make it a bit problematic to distinguish the solid and liquid aggregate states of metal clusters in computer simulations on the basis of the caloric curve behavior, in contrast to Lennard-Jones clusters where this distinction is significant.

Although Lennard-Jones clusters and other dielectric clusters can have the same icosahedral or fcc (face-centered cubic) ground state structures as many metal clusters, they differ considerably with respect to their low-lying configurationally excited states. As we have seen (Fig. 1a), the lowest configurationally excited state of the 13-atom Lennard-Jones cluster has the symmetry C_5, whereas configurational excitation of metal clusters typically involves changes in the positions of many atoms with low barriers between various structures, and, as a result, is really a mixture of many excited low-lying configurationally excited states. Next, as appears from the above, the number of lower excited states in the 13-atom Lennard-Jones cluster at zero temperature equals $12 \times 15 = 180$, where 12 is the number of cluster atoms on the external atomic shell, and 15 is the number of positions of a promoted atom on the cluster surface where it is located in a hollow in contact with three surface atoms. In the metal case, the number of low-energy configurationally excited states is far more, typically on the order of 1000 [89].

Note that the occurrence of a solid – liquid phase transition in metal clusters requires the global energy minimum to be separated by an energy gap from lower excited states. Table 4 gives the total binding energy of atoms, E_b, at zero

Table 4. The binding energy E_b of cluster atoms and configurational excitation energy ΔE for some 13-atom metal clusters.

Cluster	Ni_{13}	Ag_{13}	Au_{13}
E_b, eV	44.11	27.87	41.96
$\Delta\varepsilon$, eV	0.73	0.66	0.11
$\Delta\varepsilon/E_b$, %	1.6	2.4	0.26

temperature and the excitation energy ΔE of the lowest configurationally excited state for some 13-atom metal clusters as derived from numerical simulations [89]. In all these cases, the lowest state corresponds to the icosahedral configuration of cluster atoms.

Let us now analyze the character of melting for the Ag_{13} cluster using the data of simulations. Its caloric curve shown in Fig. 12 [89] is characterized by the melting point $T_m = 820$ K, and the cluster excitation energy at the melting point is $E_{ex} = 2.89$ eV. Note that the binding energy of this cluster amounts to 2.144 eV per atom, less than $\varepsilon_b = E_b/n = 2.87$ eV for bulk silver. This relation between the atom binding energy for a cluster and bulk systems is of course consistent with the classical expectation for small systems [104]. It is difficult to find the cluster fusion energy from the caloric curve, and we take it to be proportional to the atomic binding energy. Estimated in this way, the cluster fusion energy according to the data of Tables 3 and 4 is 0.090 eV per atom or 1.16 eV per cluster. Next, the total kinetic energy of cluster atoms for the solid aggregate state at the melting point is $E_{kin} = 1.16$ eV, as follows from the kinetic definition of temperature. Thus, we obtain the value of the anharmonicity parameter $\eta = E_{kin}/E_{ex} = 0.40$ at the melting point. This value coincides with that of the Lennard-Jones cluster ($\eta = 0.39$) within the accuracy limits of these values. For comparison, it should be indicated that for the Lennard-Jones cluster of 13 atoms we have $E_b = 44.34D$, $\Delta\varepsilon = 2.86D$, and $\Delta\varepsilon/E_b = 6.4\%$.

On the basis of the above results, one can outline the character of change of cluster parameters at the melting point T_m. We take the relationship between cluster parameters at the melting point in the standard form

$$\Delta S = \ln g\,(E_{ex}, T_m) = \frac{\Delta E}{T_m}\,, \tag{3.19}$$

where ΔS is the entropy jump in the phase transition, and $g(E_{ex})$ is the ratio of the statistical weights for the liquid and solid aggregate states at the melting point. Taking the fusion energy $\Delta E = 1.16$ eV for the cluster Ag_{13}, we find $\Delta S = 16.4$ from formula (3.19) at the melting point or, correspondingly, the number of participating liquid states $g = 1.3 \times 10^7$. This value is several orders of magnitude higher than the number of configurational excitations, which is about 10^3 (the total potential energy of cluster atoms is $U = 0.6E_{ex} = 1.72$ eV). From this it follows that the thermal motion of atoms plays a significantly greater role in a metal cluster than in a Lennard-Jones cluster.

Basing our analysis on computer simulations of 13-atom metal clusters [70, 71, 75, 89], the following simple model can be suggested for the phase transition of metal clusters, resulting from the positions of the potential curves in Fig. 10b. The liquid state includes all the configurationally excited states whose excitation energies lie below a given one. The connection between the cluster excitation energy E_{ex} and the number of configurational states n whose excitation energy is below the indicated one is given by

$$E_{ex} = \Delta E + \varepsilon\frac{n - n_{max}}{2}\,, \quad n \leqslant n_{max}\,. \tag{3.20}$$

On the basis of this dependence, one can construct the partition function for the liquid state as

$$Z_{liq} = Z_{th}\int \exp\left(-\frac{E_{ex}}{T}\right) dn = Z_{th}\exp\left(-\frac{\Delta E}{T}\right) F\left(\frac{\varepsilon}{2T}\right),$$

$$F(x) = \frac{1}{x\cosh x}\,. \tag{3.21}$$

Here, Z_{th} is the part of the partition function related to the thermal motion of atoms in the liquid state with respect to the solid one. Treating the caloric curves [89] for the isothermal case and using the energy dependence (3.20) of the isomer number allow us to separate the parts of the entropy jump at melting due to configurational excitation and to thermal atomic motion in the liquid state; these data are given in Table 5. Note that the contribution of the thermal part to the entropy jump is less for metal clusters than for Lennard-Jones clusters. According to this model, the properties of the liquid state vary sensitively with temperature, while classical thermodynamics would attribute constant parameters to the liquid aggregate state in the region of the melting point.

Table 5. Parameters of the phase transition for 13-atom metal clusters.

Cluster	Ni_{13}	Ag_{13}	Au_{13}
T_m, K	860	420	440
ΔE, eV	1.5	1.5	0.68
δT_m, K	200	60	400
ΔS_0	6.4	7.1	7.2
ΔS_m	20	41	18
$\Delta S_0/\Delta S_m$, %	32	17	40

Thus, in comparing the melting of Lennard-Jones and metal clusters, especially with regard to their differences, we have an analogy in configurational excitation from the energy standpoint. Indeed, for both cases, the liquid state is separated from the solid one by an energy gap, and the configurations of their atoms change as a result of melting. But the number of configurations that are available for liquid metal cluster increases very rapidly with an increase in the excitation energy, while the number of atomic configurations available for molten Lennard-Jones clusters remains relatively constant in the temperature range nearby the melting point. This leads to quite different behavior of entropy jumps and different relative fusion energies in these cases. Nevertheless, in spite of their differences, the phase transitions for Lennard-Jones and metal clusters may be considered from the same standpoint.

As for the methods applied to simulate Lennard-Jones and metal clusters, one can conclude that coexistence of phases, and the consequent recognition of separate, distinguishable solid and liquid forms, allows us to understand in a deepened way the character of the phase transition and, in particular, to find the temperature dependence for the entropy jump in the range of the phase transition. The absence of phase separation in computer simulations of metal clusters gives us only a rough picture of the phase transition in this case.

3.3 Character of phase coexistence in 13-atom clusters

In this analysis we shall consider clusters consisting of 13 atoms as convenient objects for describing the phase coexistence in phase transitions, since in this case we have the maximum relative range of phase coexistence because of a significant energy gap between the ground and configurationally excited states. In addition, 13 is a magic number of cluster atoms, corresponding to a completed icosahedral structure. Nevertheless, phase coexistence is also a general property of clusters of other sizes, although for a 13-atom cluster it is particularly striking.

Figure 14a exhibits the size dependence of the melting point for Lennard-Jones clusters [105], and the temperature range of phase coexistence is indicated in each case. The maximum melting points correspond to completed atomic shells ($n = 13, 19$). Moreover, these 'magic number' sizes exhibit particularly wide coexistence ranges, compared with clusters of other sizes. By contrast, for Lennard-Jones clusters consisting of 8, 14, and 17 atoms, coexistence of phases is not observed [56], i.e., the distribution functions of clusters over the total kinetic or potential energies according to computer simulations are characterized by single maxima. One can explain this difference by the character of the corresponding configurational excitation. Indeed, comparing clusters of 13 and 14 atoms and defining the liquid aggregate state as that in which an atom can move over the cluster surface freely, we reveal that an atomic transition onto the cluster surface gives the entropy jump $\Delta S = \ln(12 \times 15) = 5.2$ for a 13-atom cluster, while the entropy jump is significantly less for a 14-atom cluster. Hence, in the latter case we have an apparently smooth entropy change with cluster excitation, i.e., phase coexistence is absent or occurs too rapidly for thermal equilibration of each phase in this case. Thus, the character of phase coexistence depends on the cluster structure and the character of configurational excitation. The 17-atom cluster requires a rather different explanation from this standpoint; in this case, the solid and liquid states were not separately identifiable because passage between them seemed very labile. (More recent and precise simulations may in fact show phase coexistence for the 17-particle cluster, but with only brief dwell times in each phase.)

In this context, the question arises of just what the liquid aggregate state is for clusters. We were faced previously with different definitions, depending on the property under consideration. In considering a 13-atom cluster, we have taken this state as a configurationally excited state, as shown in Fig. 1a. From the other standpoint, we took the liquid state as the state with a high mobility of the surface atom or atoms. Evidently, this definition may be considered as a general definition of the liquid state, at least for the surface layer. From this standpoint, a surface atom of a 14-atom cluster in the liquid state moves freely over the cluster surface, while it is locked in a surface well between three surface atoms in the solid aggregate state. Then in this case, an increase in the temperature or the energy of the surface atom mobilizes that atom and allows the surface atom to pass among neighboring surface wells. Here, we would say that coexistence of phases is not a simple 2-state situation, i.e., the cluster may be found in one aggregate state, solid or liquid surface, depending on the average energy of the surface atom. At higher temperatures, the core atoms become mobile and one can observe a liquid state for the entire cluster. In the case of the 13-atom cluster, the transition of a surface atom onto the cluster surface establishes the solid – liquid transition, and the phase coexistence takes place for this cluster in some range of temperatures or cluster excitation energies.

It is necessary to distinguish 'true' melting from what we shall call 'surface melting'. In the case of clusters consisting of 13 and 14 atoms, surface melting is realized, and an atom or atoms have a high mobility on the cluster surface. Surface melting is more evident in larger clusters, with two or more shells [26, 27, 106], and also in bulk atomic systems. The 'true' melting is determined by internal atoms and is not so vivid as surface melting. The volume of an atomic system in the liquid state is greater than that for the solid. An increase in the volume per atom leads to an increase of the entropy of this atomic system and simultaneously to a decrease of the binding energy. One can infer the optimal size of this atomic system with respect to its chemical potential. The corresponding state, stable or metastable, differs from the solid state and is indeed the liquid state. From this consideration it follows that the existence of the liquid state requires definite conditions. In particular, within the framework of the void model for configurational excitation of clusters, these requirements are formulated in monograph [32].

Evidently, the definition of the liquid state, based on a high atomic mobility, is analogous to the generalized Lindemann criterion. Indeed, the Lindemann criterion [100] for simple atomic systems with a pairwise atomic interaction postulates that the solid – liquid phase transition occurs when nuclear vibrations reach an amplitude that is 10 – 15% of the equilibrium distance between nearest neighbors. In general-

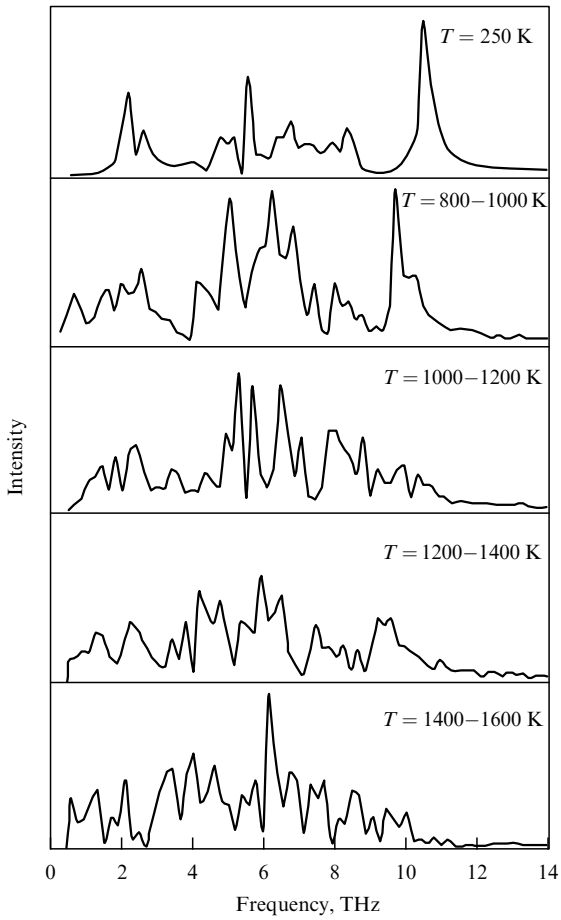

Figure 15. The vibrational spectra of the cluster Al_{13}^- at different temperatures [78].

izing the Lindemann criterion [100], the vibrational amplitude of each atom is replaced by fluctuations of bonds between nearest neighbors [21–23, 102, 103], i.e., correlations in the positions of nearest neighbors. Usually, the relative square root of the fluctuation for the square of distances between nearest neighbors, averaged over the positions of all atoms and given by formula (3.18), is used for this goal. This quantity is taken for a certain time scale, when atoms change their positions in the liquid states, and conserve these positions in the solid state. Then, the phase transition leads to a large increase of the parameter δ, as shown in Fig. 13.

Let us consider the liquid cluster aggregate state from another standpoint. If a cluster is found in the solid aggregate state, atoms oscillate in their wells, and the characteristic oscillation frequencies, broadened as they may be due to thermal atom motion, change weakly as the cluster is excited. Transition to the liquid state is accompanied by a change in the spectrum of cluster vibrations. This is demonstrated in Fig. 15, in which the vibrational spectrum of the cluster Al_{13}^{-} is given at several temperatures [78]. This shows that the cluster's characteristic frequencies vary with temperature. This example also shows that the concept of the potential energy surface is not suitable for liquid metal clusters because of mixing of atomic configurations in the many excited states, including the low-lying electronic states. Therefore, the vibrational spectra of liquid metal clusters vary significantly with variations of the cluster temperature or the degree of excitation.

4. Phase transitions in large dielectric clusters

4.1 Phase coexistence in dielectric clusters

The specific phenomenon of coexistence of the solid and liquid phases is most striking for clusters consisting of 13 atoms, when interaction between nearest neighbors dominates. In particular, this effect was discovered for the 13-atom Lennard-Jones cluster [23–25, 27, 28]. In this case, the average residence time in each aggregate state in the range of phase coexistence is long compared to a typical time of passage between phases, and the relative probability that a cluster will be located in each aggregate state determines (or reveals) thermodynamic parameters that follow from averaging these parameters over long times. For larger clusters, phase coexistence changes its character somewhat, becoming more complex, so the 13-atom cluster is perhaps the best candidate to elucidate the phase coexistence in a simple form, for two reasons [31, 32]. First, the solid state of this cluster corresponds to the completed icosahedral structure with one filled shell, and the icosahedral structure is significantly more favored than others because all the surface atoms are found in identical positions. Therefore, this cluster ground state is separated from the first configurationally excited state by a large energy gap that provides a large lifetime of each aggregate state compared with the time of transition between these states. Second, because a large fraction of atoms occupy the cluster's shell, the phase transition is characterized by a large entropy jump and therefore proceeds at low temperatures. This decreases the rate of transition between aggregate states and increases the lifetime for each aggregate state under given conditions.

Let us represent a general principle of phase coexistence that the lifetime in each aggregate state exceeds significantly the time of transition between these aggregate states. The lifetime of an aggregate state is inversely proportional to the rate of transition between these states, which in turn is proportional to $\exp(-E_a/T)$, where E_a is the activation energy for a given transition that exceeds the energy difference ΔE between states (here, in this crude approximation, we neglect the energies of the transition states above the initial minima), and T is the cluster temperature expressed in energy units. A typical time of transition between aggregate states is the time of rearrangement of the atomic configuration that changes from one aggregate state to another. This is a typical time of atomic displacement over distances of the order of a distance between nearest neighbors. We estimate the order of magnitude of this time as ~ 1 ps, and this depends weakly on temperature. Thus, the criterion of phase coexistence is fulfilled if the energy gap between aggregate states significantly exceeds the thermal atomic energy that provides a long cluster location in each aggregate state compared to a time of free displacement of atoms over atomic distances. Therefore, the concept of phase coexistence is applicable to clusters of various sizes, including macroscopic atomic systems, for which the energy of excitation of an aggregate state exceeds the thermal atomic energy at the melting point. It is quite another matter that the range of phase coexistence becomes very narrow for large clusters, which makes this effect unobservable, although the fundamental meaning still holds, in principle, for large systems.

We now consider the peculiarities of the phase transitions in large dielectric clusters in which interactions between nearest neighbors dominate. They differ from the 13-atom cluster in two ways [32]: the possibility of several aggregate states, and large fluctuations of parameters for each aggregate state, which are comparable to or exceed the energy gap between these states. Let us take as an example for demonstration of these peculiarities a 55-atom Lennard-Jones cluster for which various aspects of the phase transition were studied [26, 27, 107–112]. This cluster has a completed icosahedral structure that is separated from the lowest excited configurational state by a moderately wide energy gap, guaranteeing a long lifetime for the ground state and excited states and leading to phase coexistence. But, in contrast to the 13-atom cluster, we have in this case several aggregate states. Indeed, a 55-atom cluster with a dominant nearest-neighbor interaction has an icosahedral structure with one central atom, 12 atoms in an internal shell, and 42 atoms in an external shell. For this structure, one can identify three aggregate states [27, 111] in the caloric curve (the temperature dependence for the internal cluster energy). The first and lowest-energy is the solid state, the ground configurational state. The second aggregate state is characterized by a solid internal atom shell and liquid outer shell, and the third aggregate state is the liquid cluster state.

Another peculiarity of aggregate states of the 55-atom Lennard-Jones cluster is connected with large fluctuations of parameters for each aggregate state. Figures 4b, 4c contain the time dependences for the total potential energy of a 13-atom Lennard-Jones cluster under different external conditions, and the corresponding dependences can be obtained for the total kinetic energies of cluster atoms. These dependences were generated from computer simulations by methods of molecular dynamics in which mean values of the desired quantities are extracted at each successive short time interval, typically the time of a few vibrational periods. These data allow us to distinguish the aggregate state for cluster location at each short time interval. It is possible to construct the same

dependence for clusters of other sizes, e.g., a 55-atom cluster, but the results are typically somewhat more complicated. For example, for Lennard-Jones clusters of roughly 50 atoms, one can distinguish solid, liquid, and intermediate, 'surface-melted' phases from the simulation data [26, 27, 106]. The parameters from each of these phases could, in principle, be extracted from molecular dynamics simulations.

One can determine the phase transition parameters in another way. Specifically, the temperature range of phase coexistence is the temperature range for the resonance-like peak in the temperature dependence for the cluster's heat capacity under isothermal conditions. The transition between aggregate states in a phase coexistence range is characterized by a change of atomic configuration for this cluster established by atomic positions. In the case of a 55-atom Lennard-Jones cluster, the first configurationally excited aggregate state is characterized by 5 – 7 promoted atoms [32], which are promoted from the outer atomic shell to the cluster surface. These atoms are termed 'floaters' [26, 110] and they arise and disappear over the cluster surface.

4.2 Character of the melting of dielectric clusters

Depending on the behavior of the potential energy surface (PES) for cluster atoms, we divide clusters into two groups. In dielectric clusters for which a short-range interaction, i.e., interaction between nearest neighbors, dominates, an excited aggregate state is characterized by a restricted number of local minima of the PES, and until a cluster moves to a different excited aggregate state as the result of a change of the cluster temperature, the cluster's location in the initial set of local minima of the PES is conserved. By contrast, metal clusters at low temperatures have many excited local minima of their PESs with approximately the same excitation energy, and the cluster configurational state that is described by the distribution of occupancies of local minima of the PES varies very sensitively in the course of temperature change. We here consider dielectric clusters.

Let us analyze the character of phase coexistence in large dielectric clusters on the basis of the above data. Strictly, the range of coexistence is the full range between the low temperature at which the liquid loses its local stability, the freezing limit, and the higher temperature at which the solid loses its local stability, the melting limit [25, 28]. Nonetheless, here we take for definiteness, convenience, and especially as a way to estimate the practical observability of the coexisting phases, the range of phase coexistence such that

$$0.1 \leqslant p \leqslant 10\,, \tag{4.1}$$

where the parameter p is given by the formula

$$p = \frac{w_{\mathrm{liq}}}{w_{\mathrm{sol}}} = \exp\left(-\frac{\Delta E}{T} - \Delta S\right), \tag{4.2}$$

and w_{sol} and w_{liq} are the probabilities of a cluster residing in the solid and liquid states at this temperature, respectively, ΔE is the change of the internal cluster energy as a result of the phase transition, and ΔS is the entropy jump. Introducing the width of the coexistence range as

$$\delta T = T_1 - T_2\,,$$

where $p(T_2) = 0.1$, and $p(T_1) = 10$, we obtain

$$\delta T \approx \frac{5}{\Delta S}\,, \tag{4.3}$$

where ΔS is the entropy jump at the melting point.

Let us apply formulas (4.1) – (4.3) to the 13-atom Lennard-Jones cluster with argon parameters. In considering isothermal conditions (with the cluster in a Gibbsian canonical ensemble), taking the melting point to be $T_{\mathrm{m}} = 37$ K and the entropy jump at the melting point $\Delta S \approx 9$, we find coexistence of phases in the temperature range 28 – 46 K according to formula (4.3). For a nickel cluster of 13 atoms with the melting point $T_{\mathrm{m}} = 860$ K and the melting parameters according to Table 5, we have on the basis of formula (4.3) that the phase coexistence takes place throughout the temperature range 740 – 980 K. Next, for the Lennard-Jones cluster of 55 atoms with argon parameters we have for the melting point $T_{\mathrm{m}} = 44$ K and the entropy jump at the melting point $\Delta S = 45 \pm 2$. In this case, the phase coexistence according to formulas (4.1) and (4.3) occurs in the range 40 – 48 K. One can see that the range of readily observable phase coexistence for metal clusters is proportionately narrower than that for dielectric clusters but is nonetheless very observable, and the range of observable coexistence is wider for small clusters than for large clusters. As follows from these estimates, phase coexistence is important for small dielectric clusters when the number of cluster atoms is below 100 [1].

4.3 Role of the anharmonicity of atomic vibrations in cluster melting

In the analysis of the 13-atom Lennard-Jones cluster, we emphasized the important role of the anharmonicity of atomic vibrations for the phase transition. Indeed, the upper state of the phase transition corresponds to the more rarified atomic distribution, and the anharmonicity of atomic vibrations in this state is certainly greater than that for the lower-energy solid state. Therefore, the temperature dependence of the transition entropy in the range of the phase transition can be connected with the anharmonicity of atomic vibrations in the upper aggregate state. Note that the anharmonicity of the 13-atom Lennard-Jones clusters, as follows from an analysis of computer MD simulations [23], is relatively small [57]. Nevertheless, it is important for the behavior of the entropy jump in the range of phase coexistence [31, 32].

For larger clusters, the contribution of the anharmonicity of atomic vibrations to thermodynamic parameters in the phase transition range is determined by the anharmonicities of the potential wells, rather than the valley regions of the PES [112]. The influence of the anharmonic character of atomic vibrations on some thermodynamic parameters is given in Table 6. Evaluations were fulfilled for the Lennard-Jones cluster of n atoms with completed icosahedral shells. The

Table 6. The role of the anharmonicity of atomic vibrations in clusters for the thermodynamic parameters of two Lennard-Jones clusters LJ_n with completed icosahedral shells under isothermal conditions [112].

Cluster	T_{m}, D	L_{m}, D
LJ_{13}, harm.	0.35	2.9
LJ_{13}, anharm.	0.29	3.7
LJ_{55}, harm.	0.34	13
LJ_{55}, anharm.	0.30	16

Here, T_{m} is the melting point expressed in units of the binding energies per bond, and L_{m} is the energy difference of the two phases in the caloric curve at the melting point.

[1] *Note added in proof*: see Berry R S, Smirnov B M *Int. J. Mass. Spectr.* **280** 2004 (2009)

contribution due to the anharmonicity of atomic vibrations to the cluster parameters depends on the character of atomic interactions in this cluster [66, 113].

The role of the quantum character of atomic vibrations in the phase transition has been studied in Ref. [114] for Lennard-Jones clusters consisting of 19, 31, 38, and 55 atoms. It follows from this analysis that whatever quantum corrections may be significant due to zero-point vibrational energies and may play an important role in mixing cluster structures when the system has an icosahedral core structure and the fcc structure on its potential surface. This method later was generalized for Lennard-Jones clusters of sizes with nonicosahedral global minima [115].

4.4 Cluster heat capacity near the melting point

The heat capacity of a cluster that is under constant energy conditions is of special interest because the heat capacity of such a cluster may be negative. It is important to recognize that in this case the temperatures of the solid (T_{sol}) and liquid (T_{liq}) aggregate states are different. But one can introduce the average cluster temperature

$$T = w_{sol} T_{sol} + w_{liq} T_{liq} , \tag{4.4}$$

where w_{sol}, w_{liq} are the probabilities of the cluster residing in the solid and liquid states, respectively. This allows us to consider an isolated cluster as a thermodynamic system that is characterized by a certain temperature. Let us represent the caloric curves (the temperature dependences for the cluster energy) for cluster aggregate states in the absence of the phase transition simply by straight lines (Fig. 16). If a cluster is heated starting from low temperatures, its temperature equals $T = T_{sol}$ at low temperatures, and $T = T_{liq}$ at high temperatures. The transition between these curves near the phase transition can give the caloric curve an S-form [49, 53], which results in a negative heat capacity in the vicinity of the melting point. The analysis [32, 49] showed the reality of this character of the caloric curve.

It should be noted that the negative cluster heat capacity near the melting point does not violate general physical principles. Indeed, the heat capacity is expressed through the derivative of the mean kinetic energy of cluster atoms with respect to the average cluster temperature, and the negative heat capacity means that an increase of the total energy of cluster atoms induced an increase in configurational excitation to regions of high potential energy, and consequently to a decrease of the total kinetic energy of the cluster atoms.

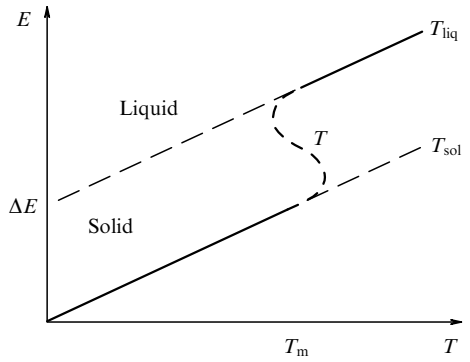

Figure 16. Caloric curves for a cluster with two aggregate states in the melting range. The S-shape transition between the straight lines related to the solid and liquid aggregate states corresponds to a negative value of the cluster heat capacity near the melting point.

Evidently, this phenomenon may even also occur for macroscopic atomic systems. In particular, in the case

$$1 \gg \frac{T_{sol} - T_{liq}}{T_{sol}} \gg \frac{1}{\sqrt{n}} , \tag{4.5}$$

where n is the number of cluster atoms, the heat capacity at the melting point is $-C_0$ [30, 32], where C_0 is the cluster heat capacity far from the melting point. Criterion (4.5) is not fulfilled for the 13-atom Lennard-Jones cluster or for many other such clusters, but the negative cluster heat capacity has been found by experiment for charged clusters of sodium [116, 117].

5. Melting and properties of metal clusters

5.1 Properties of metal clusters

Whether we are analyzing dielectric or metal clusters, we often assume that there is no electronic excitation, i.e., electrons do not partake in cluster excitation in either case. Then by analogy with dielectric clusters, one can construct the PES (potential energy surface) for a metal cluster based just on nuclear coordinates. The 13-atom clusters of the coinage metals exemplify this behavior. Computer simulations then reveal many local minima corresponding to isomers with low excitation energies (see Fig. 10b). The differences in the energies among these neighboring minima are typically small. Interparticle interactions in metal clusters are subtle and are not restricted to short ranges. This has the consequence that, in contrast to dielectric clusters for which interactions between nearest neighbors dominate, the energy gap between the ground configurational state of a metal cluster and the first configurationally excited state is, in many cases, relatively small, as are the differences in excitation energies for subsequent excited states. This leads to mixing of configurational excited states whose number increases with an increase in the excitation energy. Therefore, the liquid aggregate state of a metal cluster as a sum of a large number of configurational states changes with variation of the excitation energy. In addition, the lifetime of aggregate states of metal clusters is shorter than that for dielectric clusters, sometimes making it problematic to separate the solid and liquid aggregate states in the range of phase coexistence, as can be done for dielectric clusters.

Thus, metal clusters are characterized by similar excitation energies for neighboring configurationally excited states, and the liquid state that is composed from many excited configurational states corresponds to a varying atomic configuration in the cluster as the excitation energy varies. Taking into account the electronic degrees of freedom enhances this property of a metal cluster. Clear illustrations of this are clusters of the alkali metals, whose electronic valence shells are half-filled; that leads to an effectively continuous electronic spectrum for each nuclear configuration in principle [118]. This in turn strengthens the mixing of configurationally excited states of such a metal cluster. Therefore, interaction inside the electron subsystem and, in particular, electron–electron coupling may be vital components for describing aggregate cluster states and phase transitions between them.

Previously, we analyzed dielectric clusters as consisting of weakly interacting atoms, so that the properties of atoms are at least partially conserved in those systems in which they are bound. Now we consider metal clusters, and the first question is what clusters are actually metallic, i.e., which exhibit

properties analogous to those of bulk metals. The electrical conductivity is the most characteristic and simplest property to define membership of a given material in a category of metals. The electrical conductivities of materials vary between the limits of $10^9\ \Omega^{-1}\mathrm{cm}^{-1}$ up to $10^{-22}\ \Omega^{-1}\mathrm{cm}^{-1}$ (for example, see Refs [119 – 121]). That spans 31 orders of magnitude. The high electrical conductivities that characterize metals correspond to relatively free electron motion in these materials.

When we transfer our attention to objects the sizes of atomic clusters, other properties due to electron properties may be taken as defining metal characteristics. Physically, it is convenient to use the electron spectrum that, for a metal, is effectively continuous for low-energy electronic excitation. Indeed, the electron spectrum of bulk materials that may be interpreted as excitation energies of individual electrons consists of continuous energy bands which interact with each other and with atomic cores. For metallic atomic systems, the valence band that corresponds to valence electrons is only partially filled, i.e., electronic transitions with small energy variations are possible. When we deal with clusters, systems of a finite number of atoms, the spectrum becomes discrete; that is a general property of finite systems, both because of the small number of component atoms and because of the atomic-scale boundaries of the systems. But if the excitation energy for neighboring cluster levels is small compared to the thermal energy, one can still consider this spectrum to be continuous.

It is appropriate to start the analysis of the behavior of metal clusters from Wigner's papers [122, 123] where the importance was shown of the correlation interaction of electrons in a quantum system containing electrons and ions. This correlation energy, together with the Coulomb interaction between charged particles, determines the optimal distance between nearest neighbors in metal systems, which is described by the Wigner – Seitz radius r_W [122]. This parameter is defined such that the radius of a spherical metal particle consisting of n atoms is given by

$$r = r_{\mathrm{W}} n^{1/3}\,, \tag{5.1}$$

and the volume of a sphere of a radius r_{W} corresponds to the volume per atom of the condensed system.

This description of the electron behavior in metal clusters indicates that electrons may travel freely inside the cluster, but the correlation of electron positions is important for the cluster's structure. This aspect of electron – electron interaction is taken into account in the jellium model of metal clusters, in which the positive charge is distributed smoothly over a restricted volume determined by the cluster's physical size, and each electron resides in the field of the positive charge and a self-consistent field due to the other electrons. In this case, the electronic states are determined by the solution of the Schrödinger equation for the electron wave function that locates the electron in a self-consistent spherical field $U(r)$, where r is the electron's distance from the cluster center. Then the electronic state is characterized by the same quantum numbers as those of electrons in atoms: n is the principle quantum number; l, the orbital momentum; m, the momentum projection onto a given direction, and σ, the electron spin projection onto this direction. Correspondingly, the electron component in a cluster is distributed over shells, similar to those in atoms. The difference between the atom and jellium cluster model is such that for atoms $n \geqslant l$, whereas for a cluster the relation between positive n and l may be arbitrary. (This corresponds to the difference between hydrogenic and Sturmian functions in the Coulomb field.) Thus, the jellium model is an analogy of the self-consistent field model for atoms, and within the framework of this model cluster electrons are characterized by the same quantum numbers as those for atoms.

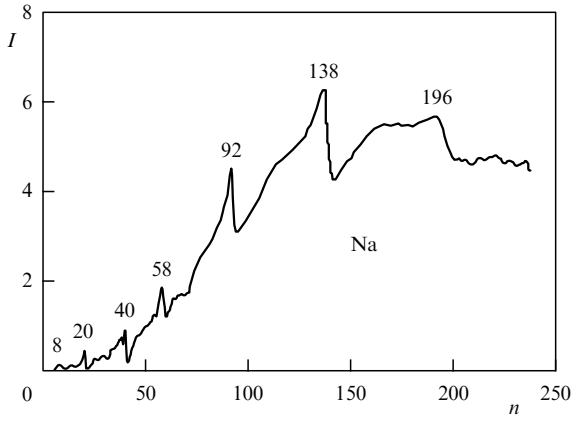

Figure 17. Mass spectrum of cluster sodium ions — the dependence of the intensity of cluster ions extracted by a field on the number of cluster atoms [128]. Intensity maxima correspond to the cluster magic numbers that are indicated.

The shell structure of a jellium cluster leads to certain magic numbers of cluster atoms — or, more precisely, of electrons — at which various cluster parameters are extremal. This structure of cluster shells is confirmed by mass spectrometry experiments (for example, see Refs [124 – 127]) for various clusters of alkali metals. Figure 17 gives the mass spectrum for sodium clusters — the dependence of the relative intensity of cluster flux on cluster size, which corresponds to the jellium model for a spherical sodium cluster [128].

The jellium model for metal clusters may have different versions due to different methods of introducing the self-consistent field that acts on electrons [118, 129 – 137]. According to the experience people have had using the jellium model, it is suitable for alkali metal clusters, and, as follows from experiments (see, for example, Refs [124, 125, 127, 138, 139]), practically identical magic numbers correspond to clusters of different alkali metals. In particular, the sequence of filling electron shells for clusters of alkali metals with the number of atoms below 100 is as follows: $1s^2 1p^6 1d^{10} 2s^2 1f^{14} 2p^6 1g^{18} 2d^{10} 3s^2 1h^{22}$ [124], if we use the notation of electron shells in atoms. As we can see, in contrast to atoms, states with low principal quantum number n can have any orbital momentum l. Note that, like electron shells in atoms, there is a competition for the filling of electronic shells in clusters. This is important for large clusters in which the sequence of filling of electron shells depends on the method of the cluster's formation. In particular, cluster heating acts on its magic numbers [127]. [2]

Just how metal-like properties develop in clusters as their size varies is a challenging aspect of the general problem of the insulator – metal transition (for example, see Refs [121, 140 – 145]). There are various methods to analyze this transition in clusters in terms of the electronic behavior. One of these is based on the size dependence of the polarizability. Indeed, the

[2] *Authors' note to English proof*: The jellium model does have limits, however; it does not give an accurate representation of aluminium clusters (see, for example, paper by Cheng H-P, Berry R S, Whetten R L *Phys. Rev. B* **43** 10647 (1991)).

polarizability of a spherical metal particle with radius R is $\alpha = R^3$ [146]; the polarizability of a dielectric particle is of course lower. In this manner, measurement of the cluster's polarizability as a function of its size allows one to find a size above which clusters become metallic and their polarizabilities vary at larger sizes close to the relation $\alpha = R^3$. This operation [147] shows that aluminium clusters become metallic when their size exceeds 40.

When an object becomes metallic and electrons can freely travel in it, the Mott–Hubbard correlation energy $U = I - EA$ becomes zero [141, 144, 148–150] (I is the ionization potential for this atomic object, and EA is the electron affinity). This corresponds to the concept of a metal with no energy gap between highest filled and lowest empty electron energy levels, HOMO and LUMO, respectively, and is realized for clusters in a form simpler than that of macroscopic systems. Moreover, this character of an insulator–metal transition, the closing of the energy gap between HOMO and LUMO, takes place both for the solid and liquid states of atomic clusters.

One can use as a criterion for the cluster's metallic state the condition that the electronic spectrum is continuous from the electronic ground state. Nevertheless, just because of the small finite size of the system, the ground state of a cluster is separated from the lowest electronic excited state by some energy gap, as demonstrated above for 13-atom clusters of coinage elements and in Fig. 10b. Therefore, atoms of simple monovalent metals form the simplest metal clusters because their electron shells are half-filled, and this leads to a nearly continuous electron spectrum for each nuclear configuration, in principle [118]. In the case of bivalent metals, an additional problem occurs regarding the continuous electron spectrum, since the metallic character of the cluster is realized only if electrons can transfer freely, presumably with only thermal energy, from the occupied valence band with $l = 0$ to the lowest empty excited levels of the spectrum with $l = 1$.

As a result, clusters of bivalent metals may have insulator properties up to some sizes, and metallic properties at larger sizes. We now consider mercury clusters from this standpoint [151]. These clusters include atoms with filled 6s shells and empty 6p shells. In clusters, atomic levels are split and, if dense enough, can be considered as broadened into bands. Mercury clusters of small sizes have occupied s^2-bands and vacant p-bands. With cluster growth, the energy of the s–p gap decreases, eventually leading to overlapping of the s- and p-bands, yielding a transition to a partially filled, effectively continuous band for the valence electrons. At that stage, the cluster becomes metallic in accordance with the Mott–Hubbard criterion. To determine the threshold of this transition, we note that a negatively charged cluster Hg_n^- has one excess electron added to a neutral mercury cluster. Then following paper [152], we compare the energy of lowest unoccupied molecular orbital (LUMO) and the energy of highest occupied molecular orbital (HOMO). Hence, measurement of the photodetachment threshold for a negatively charged cluster Hg_n^- and its comparison with the excitation energy for a neutral cluster Hg_n, as the threshold of photon absorption, allow one to determine the energy gap of the LUMO–HOMO electron transition that is analogous to the Mott–Hubbard transition for macroscopic systems. Measurement of this energy gap for clusters of small sizes and the approximation of this gap to larger clusters reveals that this gap disappears at the cluster size [151]

$$n = 400 \pm 30\,,$$

and therefore we can consider just this size as that of the dielectric–metal transition for mercury.

5.2 Interactions in metal clusters

One can divide the interaction of atoms in metal clusters into an electrostatic interaction of electrons and atomic cores, and correlation interaction between electrons [122, 123] due to coupling of valence electrons. We previously used the Sutton–Chen interaction potential [92] that accounts for the electron–electron interaction according to formulas (3.16) and (3.17), and is suitable both for metal clusters and bulk metals. There are other, related forms of this interaction, but in any case it includes both the interaction between cores for a given nuclear configuration and the interaction of the electron component, and this interaction depends on the configuration of the nuclei in the cluster. Electrons are distributed throughout the cluster volume, and the electron density at each point is self-consistent with interaction between electrons and between electrons and cores.

Let us list the interaction potentials that are used for the analysis of metal clusters. The Gupta potential [153] compares parameters of interaction inside a bound system of metal atoms with energy parameters of the bulk metal; various modifications of this potential (see, for example, Refs [154, 155]) are also employed. The tight-binding model [156] represents the interaction between cores as a sum of short-range repulsive interactions and an electron exchange interaction [157, 158]. This creates a definite band in the electronic spectrum. Including the electronic density of states in the tight-binding method leads to the second-moment approximation for the tight-binding scheme [159, 65], although this model may have other modifications [160]. The embedded atom method, based on the Voter–Chen approach, is represented in Refs [81, 161, 162]. The density functional theory with expansion of the wave functions in a basis set of plane waves [163], corresponding to the free-electron basis, is used to develop some pseudopotentials for interactions in a bound metal atom system. This form requires adopting some form of exchange interaction between electrons as, for example, was done in Ref. [164]. Various modifications of these potential forms conserve the main elements of this interaction: pair interaction between cores, Coulomb and exchange interaction between electrons, and interactions of electrons with atomic cores.

When the phase transition in clusters is analyzed by methods of molecular dynamics, the degree of order or disorder may be established on the basis of the correlation between the positions of neighboring atoms [166–170]. Let us represent the relative position r_{ik} of two neighboring atoms i and k in terms of spherical harmonics for a fixed reference frame in the form

$$Y_{lm}\left(\frac{\mathbf{r}_{ik}}{r_{ik}}\right) = Y_{lm}(\theta, \varphi)\,,$$

where θ and φ are the polar and azimuthal angles of a vector r_{ik} in the given frame of reference. Averaging over the p bonds between nearest neighbors, one can introduce an invariant for a given cluster atom i [168, 169]:

$$q_{lm}(i) = \frac{1}{p}\sum_k Y_{lm}(\theta, \varphi)\,.$$

Table 7. The second-order invariants for some bulk structures: fcc — face-centered lattice, hex — hexagonal lattice, ico — icosahedral structure, dec — decahedral structure, and liq — liquid [169].

Structure	Q_4	Q_6	Q_8
fcc	0.191	0.575	0.404
hex	0.097	0.485	0.317
ico	0	0.663	0
dec	0.053	0.430	0.139
liq	0	0	0

Averaging of the spherical harmonics over the momentum projection is done in the following way:

$$q_l(i) = \sqrt{\frac{4\pi}{2l+1} \sum_{m=-l}^{l} |q_{lm}(i)|^2}\,, \tag{5.2}$$

and then these second-order invariants are averaged over the positions of all the atoms as

$$Q_l = \langle q_l(i) \rangle\,, \tag{5.3}$$

where angle brackets mean averaging over positions of the atoms. In the same way, one can construct the third-order invariants [170].

Table 7 contains the second-order invariants for various atomic structures in clusters when only internal cluster atoms are included in averaging (5.3) [169]. On the basis of this invariant, one can determine the cluster structure. Correspondingly, in this way one can analyze cluster melting. As a demonstration of this, Fig. 18 depicts the temperature dependence for the second-order invariant Q_6 of gold clusters of different sizes, together with the temperature dependences for the binding energy per atom for these clusters. We see that cluster melting leads to a decrease in the binding energy of cluster atoms and simultaneously the second-order invariant Q_6 becomes zero for the liquid state. Therefore, determination of the second-order invariant in the course of cluster evolution via its simulation by dynamic methods allows us to determine its current aggregate state.

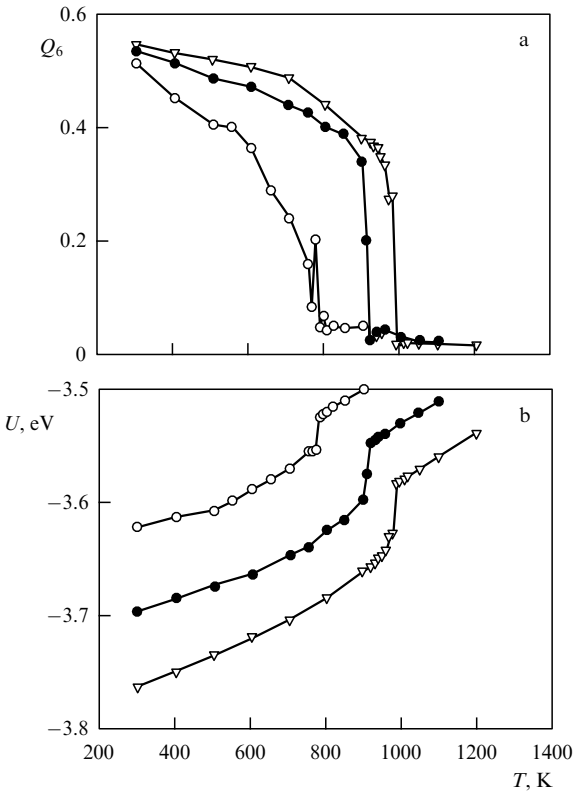

Figure 18. Temperature dependence for the second-order invariant Q_6 (a) and for the binding energy per atom (b) for gold clusters consisting of 459 atoms (open circles), 1157 atoms (closed circles) and 3943 atoms (open triangles) [169]. A stepwise change in these parameters corresponds to cluster melting.

5.3 Structures and phase transitions in gold clusters

We now consider specifically the structures and phase transitions in gold clusters among other metal clusters for several reasons. First, in 1857, Faraday [171] developed methods for creating gold nanoparticles of a given size in colloidal solutions, further advanced by Zsigmondy [172]. These systems were the vehicles for studying light scattering by small particles [173] and the character of growth of fractal aggregates [174–178]. Gold clusters play roles now in medicine [179], lithography [180], chemical catalysis [181], and nanoelectronic devices [182]. Second, relativistic effects are important for atomic interactions in gold clusters and lead to various forms of isomers as a result of structural mixing. This yields a variety of cluster structures, and hence shows the consequence of small energy differences between neighboring configurational states, including the lowest state. Therefore, in several ways, gold clusters are paragons of clusters with metallic properties. Furthermore, gold clusters exhibit chemical behavior that is strikingly different from the inert character usually associated with bulk 'noble' metals.

Gold clusters may have various structures, depending on cluster size. For small clusters, in addition to planar and polyhedral structures, zigzag and linear structures are possible [183]. These provide the highest binding energies for small clusters, those with $n < 9$; they resemble nanowires. In contrast and conflicting with that result, according to calculations [87], gold clusters of 7 atoms have a planar structure in the ground configurational state. This may also be so for $n = 4 - 11$ [87] and even for liquid-state clusters [184]. Gold clusters of dozens of atoms, in addition to planar and 3D structures including icosahedral ones, can also have cagelike and tubelike structures [183, 185, 186]. The variety of structures for gold clusters determines their catalytic properties because the favored structure may change as a result of interaction with gaseous molecules, and with it, presumably, the chemical behavior as well. We can only conclude from the information at hand that small gold clusters may assume many structures, and which are found probably depends sensitively on the conditions of formation and the environment.

The variety of structures for gold clusters is confirmed by experimental studies. In particular, one of the magic numbers for the icosahedral structure is 55, corresponding to two completed shells of this structure. Indeed, 55 is the magic number for Ag_{55}^-, but not for Au_{55}^-, according to mass-spectrometer measurements [187, 188]. The same conclusion follows from high-resolution UV photoelectron spectra [189] which have been obtained for mass-selected clusters Cu_n^-, Ag_n^-, and Au_n^-, with $n = 53 - 58$. Such measurements give the electron density of states in the uppermost occupied band; Fig. 19 gives some spectra taken from these measurements.

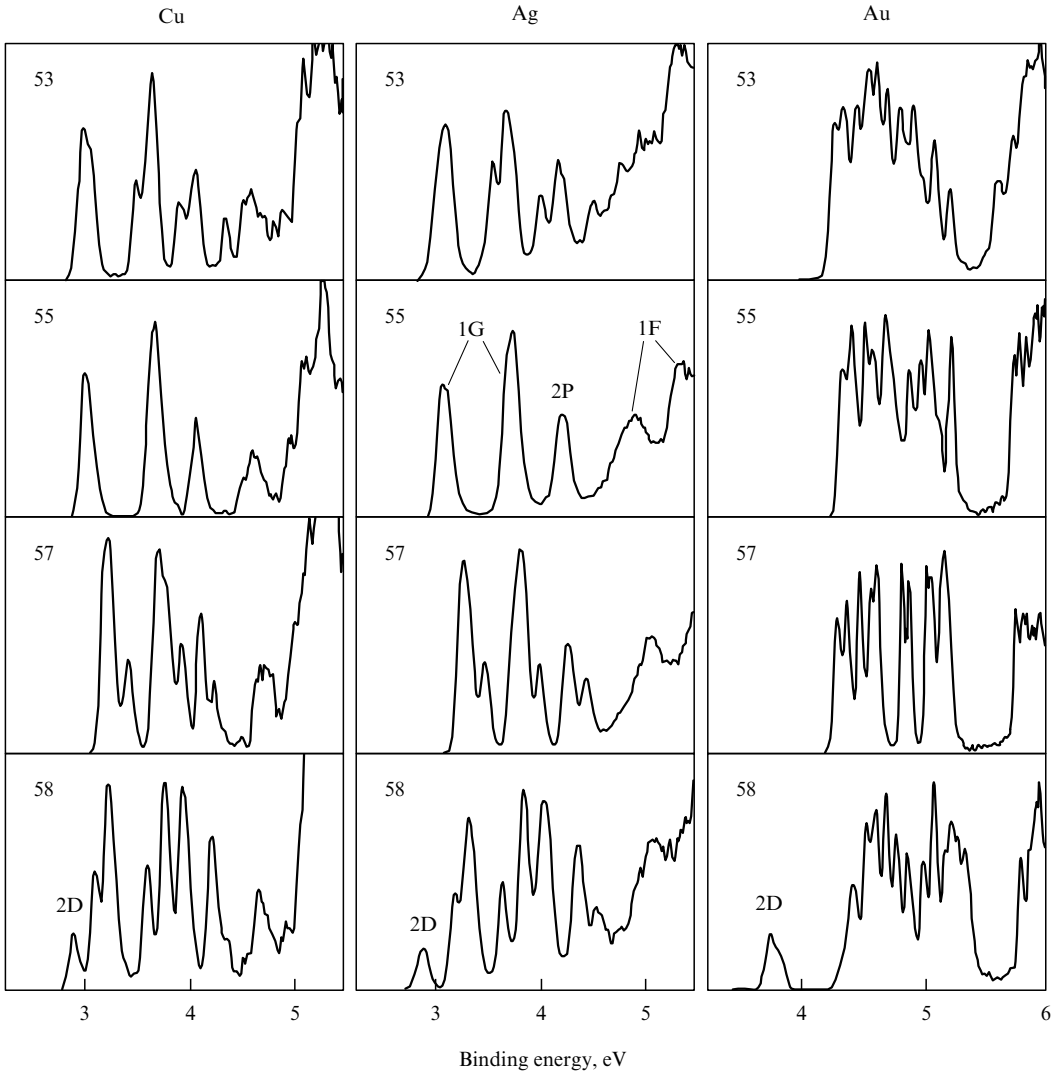

Figure 19. Photoelectron spectra of clusters Cu_n^-, Ag_n^-, Au_n^- with $n = 53$, 55, 57, 58 obtained at the cluster temperature $T = 200 \pm 50$ K and photon energy of 6.42 eV [189].

We can see that the resonant structure of these spectra gives information about the cluster structure. Comparison of each of these spectra with that calculated for a chosen cluster structure shows that only in the cases of clusters Cu_{55}^- and Ag_{55}^- is the icosahedral cluster structure realized for the ground configurational state. In the other cases of Fig. 19, including the cluster Au_{55}^-, observed spectra testify to mixtures of simple structures. Nevertheless, according to evaluations [190] on the basis of the Voter–Chen interaction potential, the ground state of the cluster Au_{54} corresponds to the icosahedral structure without the central atom.

The actual cluster structure may be determined by the method of high-resolution electron microscopy combined with computer simulations [191–197]. According to these measurements, the favored structure of gold clusters containing from hundreds up to a few thousand atoms is the truncated decahedral structure with fivefold symmetry axes or the icosahedral structure. It follows from computer simulations that the icosahedral structure becomes energetically metastable starting from sizes of dozens of atoms in a gold cluster, under thermodynamic equilibrium conditions [198, 199]. Nevertheless, computer simulation by molecular dynamics method exhibits preferential formation of the icosahedral structure for a wide range of cluster sizes [169, 170, 200]. The reason for this distinction lies, of course, in the character of the freezing process [200]. During the first stage of this process, when internal atoms are random, i.e., the core is found in the liquid state, the surface atoms form a structure with fivefold symmetry. Subsequent cluster freezing with core solidification leads to formation of the icosahedral cluster structure. Hence, the icosahedral structure of large clusters is explained by the dynamics or kinetics of the solidification process. The icosahedral structure is highly favored kinetically, even though it is not the thermodynamically most stable form. Evidently, the melting process proceeds in the same manner in the sense that the pathways for melting are the most kinetically accessible.

The specific character of the melting and freezing of gold clusters is connected with mixing of structures because various structures of gold clusters have similar excitation energies. But the character of the process of cluster solidification enhances the role of the icosahedral structures for gold clusters because this process starts from the cluster surface. Computer simulation of solidification and melting allows one

to determine the melting point depending on cluster size [169, 170, 200 – 202] and the character of the phase transition. In the course of heating, structural transformations appear at temperatures below the melting point. In particular, on the basis of computer simulations [203] of the melting process for the cluster Au_{146} with the truncated decahedron as its optimal structure, and the cluster Au_{459} with the optimal truncated octahedron structure at low temperatures, the authors of Ref. [203] concluded that precursors are formed below the melting point. Experimental study [197] by the method of high-resolution electron microscopy showed the transition between the icosahedral and decahedral cluster structures occurring at temperatures below the melting point. Moreover, this allowed constructing the phase diagram (the size dependence for transition temperatures) both for melting and for the icosahedral – decahedral structural transition for large gold clusters.

5.4 Experimental methods for the analysis of metal clusters

Computer simulation is the most powerful method for the analysis of dielectric clusters in which interaction is determined mostly by the interaction between nearest neighbors. Since experimental methods require huge resources, both material and intellectual, the contribution of experiment to studying dielectric clusters is not always a major one. For metal clusters we have another situation. First, computer simulation is not as reliable in this case as it is for dielectric clusters. In particular, this is reflected in the fact that using different models of interaction in metal clusters can lead to different atomic configurations for the solid cluster state; examples of such contradictions were given in Section 3.2. Second, because of the growing applications of metal clusters, development of experimental methods for their study has created a basis for cluster diagnostics and the technology of such applications.

Note that experimental research somehow or other does use computer simulation of clusters. In particular, Fig. 19 displays high-resolution photoelectron spectra for metal clusters containing approximately 50 atoms and separated to size. Then, the structure of each cluster follows from a comparison of measured spectra with results from numerical evaluations for different cluster structures. In the same manner, infrared (IR) cluster spectroscopy is used with results from simulation (see, for example, Refs [204 – 206]). Small neutral clusters are formed in this method in a standard manner [207 – 209] by laser irradiation of a metal rod and then they are captured by a flowing buffer gas, usually helium. The gas flow with clusters is intersected by a pulsed beam of tuned IR radiation from a laser that can excite specific cluster vibrational states. Then clusters are ionized by an excimer laser, and the mass spectrum of newly formed cluster ions allows one to ascertain what sort of cluster corresponds to the measured spectra. The composition of various clusters in a flow may be controlled by both the regime of cluster formation and the gas temperature. It is important that the absorption spectra of clusters in the IR range consist of separate resonance lines which correspond to certain identifiable vibrational transitions, and each resonance can be accompanied by the absorption of one or several photons.

The advantage of this method is that the clusters analyzed are in a gas. In particular, we give peculiarities for gold clusters Au_n, $n = 7 - 20$ in accordance with measurements [206]. In this case, the spectral range under consideration was $47 - 220\ \mathrm{cm}^{-1}$; a typical half-width of measured resonances reached $4\ \mathrm{cm}^{-1}$, while a typical line width for an infrared source was $2\ \mathrm{cm}^{-1}$. This relation allows one to distinguish spectra of clusters which contain only gold atoms from those that also hold a buffer gas atom in a cluster under observation. Such clusters may be removed from a gas flow subsequently by heating. It is natural that identification of spectra, i.e., assignment of a spectrum to a certain cluster, was established then by comparison of these spectra with those found by numerical calculations.

Another experimental method for the analysis of the structure of charged clusters is based on mobility measurements in gases for clusters of a given sort and size. In this case, basing identification on the mobility magnitude, one can discern oblong and roughly spherical cluster structures. Earlier measurements of cluster mobilities for clusters of carbon [210], silicon [211, 212], aluminium [213], and germanium [214] in helium allowed one to ascertain the possibility of distinguishing various cluster structures. In particular, it was shown in paper [213] that at some number of cluster atoms, the structures of positively charged aluminium clusters are revealed by their mobility in helium, compared with that evaluated for the hard sphere model. An increase in the helium temperature leads to transition to a structure that is close to spherical, and on the basis of the temperature dependence of the mobility of cluster ions Al_{27}^+, Al_{45}^+, and Al_{46}^+, the activation energies were found for transitions between these structures.

Let us consider the peculiarities and possibilities of this method. Cluster ions are injected into the drift chamber after selection by a mass spectrometer, i.e., they contain a specific number of atoms. Next, if there are several isomers of cluster ions at the entrance to the drift chamber, and these clusters conserve their structures in the course of drift, signals from different isomers may be separated at the chamber exit, if the signal width for one isomer is not too large. At low temperatures, one can separate signals from at least three different isomers, as observed for tin clusters Sn_n^+, $n \leqslant 68$ in helium [215]. Note that the heating-induced transition from an oblong structure to an almost spherical one may be interpreted as the transition from the solid aggregate cluster state to the liquid. Using these considerations for cluster ions Sn_n^+ with $n = 19 - 31$ gives evidence that this transition is absent at temperatures below 555 K [216], which means the melting point for these clusters is above the melting point of bulk tin, 505 K. One may immediately think that this contradicts general principles. Indeed, if a small element is cut off from a bulk system, the binding energy of atoms for this small element will be less than that for a bulk system because of surface effects. This means that the energy parameters of a cut-off element-cluster, including the cluster melting point, must be less than those for a macroscopic system. For example, in the sodium case this decrease in the melting point for clusters consisting of 55 to 357 atoms equals approximately 30% [217].

This contradiction is explained by computer simulation that, in particular, was made for the cluster Sn_{20}^+ [218]. In this case, the oblong structure that relates to the ground cluster state is a tri-capped trigonal prism structure in which the prisms are joined by bases. This structure is simply not the structure of bulk tin, i.e., this cluster cannot be cut off from bulk tin. Since this structure exhibits a higher binding energy of atoms than that of 'cut-off bulk' tin, this structure could well exhibit a melting point above that of the bulk. The nature

of the interatomic binding could, correspondingly, also differ from that of the bulk.

Analogous results were obtained for clusters Ga_n^+ with $n = 17, 39, 40$ in the temperature range $T = 90-720$ K [219]. In this case, an indirect method of increasing the internal energy of the cluster proceeds from its acceleration up to energies of several hundred electron-volts and subsequent braking in helium; this method is analogous to photoexcitation of sodium clusters [116]. Computer simulations of the clusters Ga_{13}^+, Ga_{17}^+ [221] and the clusters Ga_{30}^+, Ga_{31}^+ [221] show that a specific structure of the ground state different from that of the bulk may lead to a heightened cluster melting point, in comparison with that of a macroscopic system.

The development of experimental techniques and diagnostics for the analysis of small metal clusters paves the way for cluster applications as catalysts. The task of a catalyst is acceleration of a chemical process without consumption of the catalyst material. Typically, in the catalyzed reaction, one of the reactant molecules attaches to a catalyst and reacts with other molecules in this state. From the formal standpoint, this character of the process generally leads to a decrease in the activation energy of the process (or to an increase in the entropy of the transition state) and hence to its acceleration in this way. If the process consists of several stages, the catalyst may decrease the number of stages. Of course, one cannot generally state beforehand that a given metal may be a catalyst for a certain chemical process, although the techniques for making such predictive calculations are being developed now. Nevertheless, one can expect the coinage metals to be among the prime candidates for this because of competition of both electronic and configurational cluster structures.

Let us consider the peculiarities of utilizing metal catalysts for the simple chemical process

$$NO + CO \rightarrow \frac{1}{2}N_2 + CO_2\,, \tag{5.4}$$

for which palladium clusters Pd_n with the numbers of atoms from 4 to 30 were used as catalysts [222, 223]. One can describe a simple scheme of this process such that two molecules of NO form bonds with the cluster surface due to nitrogen atoms and then these nitrogen atoms of the NO molecules establish a bond with each other. Then as a result of collisions with CO molecules they lose oxygen atoms, and a newly formed nitrogen molecule may lose its bonds with the cluster. Palladium clusters are bonded in these experiments to an MgO surface. Mass-spectrometric cluster size selection provides a means to locate clusters of a given size on the surface, and because clusters occupy a small part of the surface (below 0.5%), one can ignore interactions between clusters.

The study of this process showed that it proceeds if the number of cluster atoms exceeds 5, sufficient to correspond to the above process scheme because two nitrogen atoms must form a bond between themselves. Next, the rate constant of this process as a temperature function has a maximum in the temperature range $400-500$ K; the interpretation of this is that at higher temperatures the NO molecules do not bond readily with the cluster surface.

Now let us discuss why clusters may be better as catalysts than a macroscopic surface of the same material. In a catalyst, a metallic property shows its worth in capturing a reacting molecule at the surface and in deceasing the potential barrier of a chemical process in this manner. Evidently, such possibilities are wider for a cluster for various reasons. The cluster has a much higher proportion of its atoms on a surface; in contrast with a bulk sample, a cluster may well exhibit a large number of isomers — configurationally excited cluster states with low excitation energies. The possibility for a cluster to change its atomic configuration in the course of a reaction gives flexibility for the system to find optimal configurations, both for the initial reaction stage when a reactant molecule is captured by the cluster, and for intermediate or final process stages when a change in cluster configuration may lead to a decrease in the reaction barrier. These conditions hold true for an atomic system in which transitions between configurational states are possible when a reacting molecule forms a bond with this atomic system. While the surfaces of both a cluster and a macroscopic atomic system are suitable as a catalyst, the cluster may have a structural flexibility unavailable to the bulk material. The optimal distance between potential wells where reacting molecules are located may be different for reagents and reaction products. Then, metal clusters which permit a change in the atomic configuration in the course of a chemical reaction may be better as catalysts than a macroscopic metal surface [224] with a single structure. Note that a cluster catalyst is more complicated than a metal surface because in a typical use of a cluster catalyst, the clusters must be attached to a macroscopic surface and form bonds with it, still conserving the individuality of the clusters. It should be emphasized that the above example (5.4) is not ideal from the standpoint of comparing cluster and surface catalysts because both large palladium clusters and bulk palladium are good catalysts for this process [225–227]. Nevertheless, this example was convenient for explanation of the process's character because of its simplicity.

Speaking in support of the standpoint that clusters are better catalysts than a macroscopic metal surface, we base our discussion on the example of CO oxidation when gold clusters on an iron oxide surface are the catalyst [228]. Then, the oxidation reaction is selective with respect to cluster size, and an optimal cluster size is on the order of ten atoms. An analogous result [229] corresponds to a low-temperature oxidation of CO formed by oxidation of hydrocarbons. This process may be considered as a result of structural transitions for gold clusters bonded with CO molecules [87]. One more example of this type relates to a fuel cell with a platinum catalyst in which oxidation of hydrocarbons (and possibly hydrogen) creates an electric potential, i.e., chemical energy is converted into electric. Then, the addition of gold clusters to the platinum surface increases the time of catalyst functioning without contaminating the catalyst [230, 231].

The technology aspect of this problem is noteworthy. In order to prepare the catalyst under consideration, it is necessary to have a specific experimental technique that includes a cluster generator with mass selection of the clusters, an atomic force microscope or a scanning electron microscope to study the cluster behavior on the surface, and diagnostic tools for the analysis of the chemical process under consideration. Although this technique exists for some systems and may even be available, such investigations become expensive. In addition, the tasks require a high qualification for specialists partaking in these investigations. Therefore, the availability of an expensive experimental technique and of qualified personnel are necessary conditions for the creation and development of cluster catalysts, i.e., we are dealing with the same requirements that relate to other spheres of science-intensive technology.

6. Conclusions

The analysis achieved by computer simulation of Lennard-Jones clusters by methods of molecular dynamics under various conditions gives a detailed representation about the evolution of cluster parameters in the course of variation of cluster temperature or excitation energy in terms of thermodynamics. Separation of the solid and liquid phases in the dynamic cluster simulation and a separate analysis under adiabatic and isothermal conditions allow us to study cluster behavior in detail in the range of phase coexistence. Passage to a thermodynamic cluster description on the basis of the results of dynamic cluster simulation gives us the possibility of analyzing cluster behavior in the phase coexistence range within the framework of simple models. Dynamic simulation of metal clusters is fulfilled without separating the solid and liquid phases. Nevertheless, the experience of cluster study in the phase transition range testifies to the paramount role of dynamic cluster simulation for gaining information about cluster behavior.

The analysis has been applied especially to treat the results of computer simulations of clusters consisting of 13 atoms. These clusters have one completed shell and an icosahedral structure for the ground configurational state, and therefore they have only one liquid state; that simplifies the analysis. In addition, the ground configurational state of these clusters (the solid aggregate state) is separated from lower excited configurational states (the liquid aggregate state) by an energy gap whose relative value is greater than that for clusters of other sizes. Therefore, for 13-atom clusters, the properties under consideration are revealed particularly clearly, in a way that simplifies the analysis and allows one to be free from concomitant effects.

The results of computer simulations for Lennard-Jones clusters of 13 atoms by methods of molecular dynamics that are made under microcanonical and canonical conditions, together with the analysis of the potential energy surface for this cluster in a multidimensional space of atomic coordinates, allow us to compose a simple model for cluster behavior in the range of dynamic phase coexistence. Namely, the aggregate states comply with atomic configurations which relate to certain local minima of the potential energy surface, and the phase transition corresponds to configurational cluster excitation due to transition between local minima of the potential energy surface. But separating the cluster's degrees of freedom into configurational and thermal ones, where the latter are associated with cluster vibrations, and then identifying the phase transition with the configurational transition, we find nevertheless that thermal atom motion plays a significant role in the phase transition. This is connected with the anharmonicity of cluster oscillations; because in the liquid state the cluster is looser than in the solid state, the different contribution to the transition entropy by the solid and liquid states determines the important contribution of atomic thermal motion to the entropy jump at cluster melting. For the 13-atom Lennard-Jones cluster, this contribution to the entropy is comparable to the contribution due to configurational excitation, whereas for metal clusters the contribution from atomic thermal motion may be even greater. Thus, different characters of atomic motion in various aggregate states may be integral to the character of the phase transition. This effect shifts the cluster's excitation energy at the melting point, if the cluster is under microcanonical conditions, in the direction of small values and allows us to connect the melting point with the character of thermal atom motion (the Lindemann criterion, etc.). In addition, this leads to a temperature dependence for the entropy jump in the range of phase coexistence, as demonstrated for the 13-atom Lennard-Jones cluster.

Comparing the behavior of the Lennard-Jones and metal clusters in the phase transition range, we find an analogy that consists in the existence of two aggregate states, the solid one and the liquid one, and these states are separated by an energy gap. But the nature of the liquid state is different for these clusters. For the 13-atom Lennard-Jones cluster, the liquid state corresponds to a simple configurational excitation that consists of the one-atom transition from the completed shell to the cluster surface, and the newly formed configuration is conserved in the course of subsequent cluster heating or excitation. In the case of metal clusters, the liquid aggregate state is a mixture of different atomic configurations in the cluster, and the number of isomers in the liquid state increases with increasing temperature. Therefore, the atomic configuration for the liquid state of a metal cluster varies with cluster excitation. In addition, the relative value of the energy gap between solid and liquid states is significantly more for Lennard-Jones clusters than for metal clusters. Hence, the contribution to the entropy of the phase transition due to configurational excitation is more striking for Lennard-Jones clusters than for metal clusters. Correspondingly, the range of phase coexistence for clusters of a given size is wider, relative to the absolute melting point, for the Lennard-Jones clusters than for metal clusters.

The variety of atomic configurations in metal clusters also reflects the role of electrons in the formation of cluster structures. Additional degrees of freedom of metal clusters due to electrons widens the number of atomic configurations that compete in the course of its evolution. Moreover, due to a high rate of transition between structures of metal clusters, the kinetics of cluster evolution is important. In particular, we learn from the study of large gold clusters that the structure of the solid cluster, resulting from cooling of a hot cluster, is determined by the kinetics of cooling and solidification of this cluster rather than by the thermodynamics of its solid aggregate state. This testifies to the complexity of processes proceeding in the course of phase transitions in metal clusters. Subsequent studies will allow us to understand in detail the character of the phase transition for various metal structures and the role of the electronic component in this phenomenon.

Experimental methods are used to a lesser degree for the study of dielectric clusters compared to metal ones for two reasons. First, computer simulation for dielectric clusters is more reliable than that for metal clusters. Second, metal clusters are of interest for applications, and therefore experimental methods may be used for diagnostics in applied problems. Experimental methods are based on applying mass spectrometric techniques, devices of IR and UV spectroscopy of high resolution, atom force electron microscopy (AFM) and scanning electron microscopy (SEM), and generators of metal clusters. Usually, the experimental study of metal clusters is combined with their computer simulation. Mastering the contemporary experimental technique is necessary for solving new applied tasks in the nanotechnology field, such as the creation of specific catalysts in which metallic clusters of a certain size and composition are fasten to a certain surface. In spite of the complexity and expense of the requisite devices for this goal, which also require highly qualified attendant

personnel, the subsequent development of this area of science and technology will progress just in this direction.

References

1. Echt O, Sattler K, Recknagel E *Phys. Rev. Lett.* **47** 1121 (1981)
2. Echt O et al. *Ber. Bunsenges. Phys. Chem.* **86** 860 (1982)
3. Ding A, Hesslich J *Chem. Phys. Lett.* **94** 54 (1983)
4. Harris I A, Kidwell R S, Northby J A *Phys. Rev. Lett.* **53** 2390 (1984)
5. Phillips J C *Chem. Rev.* **86** 619 (1986)
6. Harris I A et al. *Chem. Phys. Lett.* **130** 316 (1986)
7. Miehle W et al. *J. Chem. Phys.* **91** 5940 (1989)
8. Easter D C et al. *Chem. Phys. Lett.* **157** 277 (1989)
9. Easter D C, Whetten R L, Wessel J E *J. Chem. Phys.* **94** 3347 (1991)
10. Beck S M, Hecht J H *J. Chem. Phys.* **96** 1975 (1992)
11. Farges J et al. *Surf. Sci.* **106** 95 (1981)
12. Kim S S, Stein G D *J. Colloid. Interface Sci.* **87** 180 (1982)
13. Farges J et al. *J. Chem. Phys.* **78** 5067 (1983)
14. Farges J et al. *J. Chem. Phys.* **84** 3491 (1986)
15. Lee J W, Stein G D *J. Phys. Chem.* **91** 2450 (1987)
16. Farges J et al. *Adv. Chem. Phys.* **70** 45 (1988)
17. Bartell L S *Chem. Rev.* **86** 491 (1986)
18. Van de Waal B W *J. Chem. Phys.* **98** 4909 (1993)
19. McGinty D J *J. Chem. Phys.* **58** 4733 (1973)
20. Briant C L, Burton J J *J. Chem. Phys.* **63** 2045 (1975)
21. Etters R D, Kaelberer J *Phys. Rev. A* **11** 1068 (1975)
22. Etters R D, Kaelberer J *J. Chem. Phys.* **66** 5112 (1977)
23. Jellinek J, Beck T L, Berry R S *J. Chem. Phys.* **84** 2783 (1986)
24. Berry R S et al. *Adv. Chem. Phys.* **90** 75 (1988)
25. Berry R S *Chem. Rev.* **93** 2379 (1993)
26. Cheng H-P, Berry R S *Phys. Rev. A* **45** 7969 (1992)
27. Kunz R E, Berry R S *Phys. Rev. E* **49** 1895 (1994)
28. Berry R S, in *Theory of Atomic and Molecular Clusters*: *with a Glimpse at Experiments* (Ed. J Jellinek) (Berlin: Springer-Verlag, 1999) p. 1
29. Berry R S, Smirnov B M *Zh. Eksp. Teor. Fiz.* **127** 1282 (2005) [*JETP* **100** 1129 (2005)]
30. Berry R S, Smirnov B M *J. Non-Cryst. Solids* **351** 1543 (2005)
31. Berry R S, Smirnov B M *Usp. Fiz. Nauk* **175** 367 (2005) [*Phys. Usp.* **48** 345 (2005)]
32. Berry R S, Smirnov B M *Phase Transitions of Simple Systems* (Heidelberg: Springer-Verlag, 2008)
33. Vekhter B et al. *J. Chem. Phys.* **106** 4644 (1997)
34. Berry R S, Smirnov B M *Zh. Eksp. Teor. Fiz.* **120** 889 (2001) [*JETP* **93** 777 (2001)]
35. Gibbs J W *Trans. Conn. Acad. Arts Sci.* **3** 108 (1875); **3** 343 (1878)
36. Gibbs J W *The Collected Works* (New York: Longmans, Green and Co., 1928)
37. Lennard-Jones J E, Ingham A E *Proc. R. Soc. London A* **107** 463 (1924)
38. Lennard-Jones J E *Proc. R. Soc. London A* **106** 636 (1925)
39. Smirnov B M *Usp. Fiz. Nauk* **171** 1291 (2001) [*Phys. Usp.* **44** 1229 (2001)]
40. Smirnov B M *Principles of Statistical Physics* (Weinheim: Wiley-VCH, 2006)
41. Hoare M R, Pal P *Adv. Phys.* **20** 161 (1971); **24** 645 (1975)
42. Hoare M R *Adv. Chem. Phys.* **40** 49 (1979)
43. Stillinger F H, Weber T A *Phys. Rev. A* **25** 978 (1982)
44. Stillinger F H, Weber T A *Phys. Rev. A* **28** 2408 (1983)
45. Corti D S et al. *Phys. Rev. E* **55** 5522 (1997)
46. Ball K D, Berry R S *J. Chem. Phys.* **111** 2060 (1999)
47. Komatsuzaki T, Berry R S *J. Chem. Phys.* **110** 9160 (1999)
48. Wales D J et al. *Adv. Chem. Phys.* **115** 1 (2000)
49. Wales D J *Energy Landscapes* (Cambridge: Cambridge Univ. Press, 2003)
50. Natanson G, Amar F, Berry R S *J. Chem. Phys.* **78** 399 (1983)
51. Berry R S, Jellinek J, Natanson G *Phys. Rev. A* **30** 919 (1984); *Chem. Phys. Lett.* **107** 227 (1984)
52. Berry R S, Smirnov B M *J. Chem. Phys.* **114** 6816 (2001)
53. Bixon M, Jortner J *J. Chem. Phys.* **91** 1631 (1989)
54. Becker O M, Karplus M *J. Chem. Phys.* **106** 1495 (1997)
55. Wales D J, Berry R S *J. Chem. Phys.* **92** 4283 (1990)
56. Davies H L, Jellinek J, Berry R S *J. Chem. Phys.* **86** 6456 (1987)
57. Smirnov B M *Usp. Fiz. Nauk* **164** 1165 (1994) [*Phys. Usp.* **37** 1079 (1994)]
58. Smirnov B M *Phys. Scripta* **51** 402 (1995)
59. Honeycutt J D, Andersen H C *J. Phys. Chem.* **91** 4950 (1987)
60. Smirnov B M *Clusters and Small Particles*: *in Gases and Plasmas* (New York: Springer, 2000)
61. Smirnov B M *Plasma Chem. Plasma Process.* **13** 673 (1993)
62. Smirnov B M *Usp. Fiz. Nauk* **163** (10) 29 (1993) [*Phys. Usp.* **36** 933 (1993)]
63. Häberlen O D et al. *J. Chem. Phys.* **106** 5189 (1997)
64. Doye J P K, Wales D J *J. Chem. Soc. Faraday Trans.* **93** 4233 (1997)
65. Doye J P K, Wales D J *New J. Chem.* **22** 733 (1998)
66. Miller M A, Doye J P K, Wales D J *Phys. Rev. E* **60** 3701 (1999)
67. Wilson N T, Johnston R L *Eur. Phys. J. D* **12** 161 (2000)
68. Darby S et al. *J. Chem. Phys.* **116** 1536 (2002)
69. Wang J, Wang G, Zhao J *Phys. Rev. B* **66** 035418 (2002)
70. Arslan H, Güven M H *Acta Phys. Slovac.* **56** 511 (2006)
71. Yildirim E K, Atis M, Guvenc Z B *Phys. Scripta* **75** 111 (2007)
72. Kaiming D et al. *Phys. Rev. B* **54** 11907 (1996)
73. Zhang W et al. *J. Chem. Phys.* **121** 7717 (2004)
74. Watari N, Ohnishi S *J. Chem. Phys.* **106** 7531 (1997)
75. Sebetci A, Guvenc Z B *Modelling Simul. Mater. Sci. Eng.* **12** 1131 (2004)
76. Akola J, Häkkinen H, Manninen M *Phys. Rev. B* **58** 3601 (1998)
77. Rao B K, Khanna S N, Jena P *Phys. Rev. B* **62** 4666 (2000)
78. Akola J, Manninen M *Phys. Rev. B* **63** 193410 (2001)
79. Calleja M et al. *Phys. Rev. B* **60** 2020 (1999)
80. Reddy B V et al. *Phys. Rev. B* **59** 5214 (1999)
81. Michaelian K, Rendón N, Garzón I L *Phys. Rev. B* **60** 2000 (1999)
82. Moseler M et al. *Phys. Rev. Lett.* **86** 2545 (2001)
83. Lee Y J et al. *Phys. Rev. Lett.* **86** 999 (2001)
84. Lee Y J et al. *Comput. Phys. Commun.* **142** 201 (2001)
85. Kumar V, Kawazoe Y *Phys. Rev. B* **65** 125403 (2002)
86. Oviedo J, Palmer R E *J. Chem. Phys.* **117** 9548 (2002)
87. Fernández E M et al. *Phys. Rev. B* **70** 165403 (2004)
88. Chang C M, Chou M Y *Phys. Rev. Lett.* **93** 133401 (2004)
89. Arslan H, Güven M H *New J. Phys.* **7** 60 (2005)
90. Sakurai M et al. *J. Chem. Phys.* **111** 235 (1999)
91. Finnis M W, Sinclair J E *Philos. Mag. A* **50** 45 (1984)
92. Sutton A P, Chen J *Philos. Mag. Lett.* **61** 139 (1990)
93. Garzon I L, Jellinek J *Z. Phys. D* **20** 235 (1991)
94. Garzon I L, Jellinek J *Z. Phys. D* **26** 316 (1993)
95. Neirotti J P et al. *J. Chem. Phys.* **112** 10340 (2000)
96. Calvo F et al. *J. Chem. Phys.* **112** 10350 (2000)
97. Lee Y J et al. *J. Comput. Chem.* **21** 380 (2000)
98. Carignano M A *Chem. Phys. Lett.* **361** 291 (2002)
99. Freeman D L, Doll J D *J. Chem. Phys.* **82** 462 (1985)
100. Lindemann F A *Phys. Z.* **11** 609 (1910)
101. Hansen J-P, Verlet L *Phys. Rev.* **184** 151 (1969)
102. Kaelberer J B, Etters R D *J. Chem. Phys.* **66** 3233 (1977)
103. Zhou Y, Karplus M, Ball K D, Berry R S *J. Chem. Phys.* **116** 2323 (2002)
104. Thomson W *Philos. Mag.* **42** 448 (1871)
105. Beck T L, Jellinek J, Berry R S *J. Chem. Phys.* **87** 545 (1987)
106. Nauchitel V V, Pertsin A J *Mol. Phys.* **40** 1341 (1980)
107. Wales D J *Chem. Phys. Lett.* **166** 419 (1990)
108. Braier P A, Berry R S, Wales D J *J. Chem. Phys.* **93** 8745 (1990)
109. Labastie P, Whetten R L *Phys. Rev. Lett.* **65** 1567 (1990)
110. Cheng H P, Berry R S *MRS Symp. Proc.* **206** 241 (1991)
111. Kunz R E, Berry R S *Phys. Rev. Lett.* **71** 3987 (1993)
112. Doye J P K, Wales D J *J. Chem. Phys.* **102** 9659 (1995)
113. Ball K D, Berry R S *J. Chem. Phys.* **109** 8541 (1998)
114. Calvo F, Doye J P K, Wales D J *J. Chem. Phys.* **114** 7312 (2001)
115. Doye J P K, Calvo F *J. Chem. Phys.* **116** 8307 (2002)
116. Schmidt M et al. *Phys. Rev. Lett.* **79** 99 (1997)
117. Schmidt M et al. *Nature* **393** 238 (1998)
118. de Heer W A *Rev. Mod. Phys.* **65** 611 (1993)
119. Bardeen J *J. Appl. Phys.* **11** 88 (1940)
120. Ehrenreich H *Sci. Am.* **217** 195 (1967)
121. Edwards P P et al. *Philos. Trans. R. Soc. London* **356** 5 (1998)
122. Wigner E P, Seitz F *Phys. Rev.* **46** 509 (1934)
123. Wigner E *Phys. Rev.* **46** 1002 (1934)
124. Knight W D et al. *Phys. Rev. Lett.* **52** 2141 (1984)

125. Pedersen J et al. *Nature* **353** 733 (1991)
126. Martin T P et al. *Z. Phys. D* **19** 25 (1991)
127. Bréchignac C et al. *Phys. Rev. B* **47** 2271 (1993)
128. Bjørnholm S et al. *Phys. Rev. Lett.* **65** 1627 (1990)
129. Beck D E *Phys. Rev. B* **35** 7325 (1987)
130. Ekardt W *Phys. Rev. B* **29** 1558 (1984)
131. Ekardt W *Phys. Rev. B* **31** 6360 (1985)
132. Chou M Y, Cohen M L *Phys. Lett. A* **113** 420 (1986)
133. Yannouleas C et al. *Phys. Rev. Lett.* **63** 255 (1989)
134. Brack M *Phys. Rev. B* **39** 3533 (1989)
135. Nishioka H, Hansen K, Mottelson B R *Phys. Rev. B* **42** 9377 (1990)
136. Bertsch G *Comput. Phys. Commun.* **60** 247 (1990)
137. Genzken O, Brack M *Phys. Rev. Lett.* **67** 3286 (1991)
138. Martin T P et al. *Chem. Phys. Lett.* **172** 209 (1990)
139. Martin T P et al. *Chem. Phys. Lett.* **186** 53 (1991)
140. Herzfeld K F *Phys. Rev.* **29** 701 (1927)
141. Mott N F *Metal-Insulator Transitions* (London: Taylor & Francis, 1974)
142. Edwards P P, Sienko M J *Int. Rev. Phys. Chem.* **3** 83 (1983)
143. Pauling L *J. Solid State Chem.* **54** 297 (1984)
144. Mott N F *Metal-Insulator Transitions* 2nd ed. (London: Taylor & Francis, 1990)
145. Ashcroft N W *J. Non-Cryst. Solids* **156** 621 (1993)
146. Landau L D, Lifshitz E *Elektrodinamika Sploshnykh Sred* (Electrodynamics of Continuous Media) (Moscow: Nauka, 1982) [Translated into English (Oxford: Pergamon Press, 1984)]
147. de Heer W, Milani P, Chtelain A *Phys. Rev. Lett.* **63** 2834 (1989)
148. Hubbard J *Proc. R. Soc. London A* **276** 238 (1963)
149. Hubbard J *Proc. R. Soc. London A* **277** 237 (1964)
150. Hubbard J *Proc. R. Soc. London A* **281** 401 (1964)
151. Busani R, Folkers M, Cheshnovsky O *Phys. Rev. Lett.* **81** 3836 (1998)
152. Cheshnovsky O et al. *Chem. Phys. Lett.* **138** 119 (1987)
153. Gupta R P *Phys. Rev. B* **23** 6265 (1981)
154. Tománek D, Mukherjee S, Bennemann K H *Phys. Rev. B* **28** 665 (1983)
155. Sawada S, Sugano S *Z. Phys. D* **14** 247 (1989)
156. Friedel, in *Electrons* Vol. 1 *Physics of Metals* (Ed. J M Ziman) (New York: Pergamon Press, 1969)
157. Chadi D J *Phys. Rev. B* **19** 2074 (1979)
158. Sutton A P et al. *J. Phys. C: Solid State Phys.* **21** 35 (1988)
159. Cleri F, Rosato V *Phys. Rev. B* **48** 22 (1993)
160. Koskinen P *New J. Phys.* **8** 9 (2006)
161. Daw M S, Baskes M I *Phys. Rev. Lett.* **50** 1285 (1983)
162. Daw M S, Baskes M I *Phys. Rev. B* **29** 6443 (1984)
163. Payne M C et al. *Rev. Mod. Phys.* **64** 1045 (1992)
164. Perdew J P et al. *Phys. Rev. B* **46** 6671 (1992)
165. Baletto F, Ferrando R *Rev. Mod. Phys.* **77** 371 (2005)
166. Steinhardt P J, Nelson D R, Ronchetti M *Phys. Rev. B* **28** 784 (1983)
167. Quirke N *Mol. Simul.* **1** 249 (1988)
168. Chushak Y, Bartell L S *J. Phys. Chem. A* **104** 9328 (2000)
169. Chushak Y G, Bartell L S *J. Phys. Chem. B* **105** 11605 (2001)
170. Wang Y, Teitel S, Dellago C *J. Chem. Phys.* **122** 214722 (2005)
171. Faraday M *Philos. Trans.* **147** 152 (1857)
172. Zsigmondy R *Lieb. Ann. Chem.* **301** 30 (1898)
173. Steubing W *Ann. Physik* **24** 1 (1907); **26** 329 (1908)
174. Weitz D A, Oliveria M *Phys. Rev. Lett.* **52** 1433 (1984)
175. Weitz D A et al. *Phys. Rev. Lett.* **53** 1657 (1984)
176. Weitz D A et al. *Phys. Rev. Lett.* **54** 1416 (1985)
177. Keefer K D, Schaefer D W *Phys. Rev. Lett.* **56** 2376 (1986)
178. Wilcoxon J P, Martin J E, Schaefer D W *Phys. Rev. A* **39** 2675 (1989)
179. Weiser H B *Colloid Chemistry* (New York: J. Wiley, 1939)
180. Zheng J, Chen Z, Liu Z *Langmuir* **16** 9673 (2000)
181. Bell A T *Science* **299** 1688 (2003)
182. Xiao Y et al. *Science* **299** 1877 (2003)
183. Xiao L et al. *J. Chem. Phys.* **124** 114309 (2006)
184. Koskinen P et al *Phys. Rev. Lett.* **98** 015701 (2007)
185. Gu X et al. *Phys. Rev. B* **70** 205401 (2004)
186. Fa W, Dong J *J. Chem. Phys.* **124** 114310 (2006)
187. Krückeberg S et al. *Eur. Phys. J. D* **9** 169 (1999)
188. Herlert A et al. *J. Electron Spectrosc. Relat. Phenom.* **106** 179 (2000)
189. Häkkinen H et al. *Phys. Rev. Lett.* **93** 093401 (2004)
190. Alamanova D, Grygoryan V G, Springborg M *Z. Phys. Chem.* **220** 811 (2006)
191. Komoda T *Jpn. J. Appl. Phys.* **7** 27 (1968)
192. Buffat P-A et al. *Faraday Discuss.* **92** 173 (1991)
193. Marks L D *Rep. Prog. Phys.* **57** 603 (1994)
194. Ascencio J A et al. *Surf. Sci.* **396** 349 (1998)
195. Ascencio J A, Pérez M, José-Yacamán M *Surf. Sci.* **447** 73 (2000)
196. Koga K, Sugawara K *Surf. Sci.* **529** 23 (2003)
197. Koga K, Ikeshoji T, Sugawara K *Phys. Rev. Lett.* **92** 115507 (2004)
198. Cleveland C L et al. *Phys. Rev. Lett.* **79** 1873 (1997)
199. Baletto F et al. *J. Chem. Phys.* **116** 3856 (2002)
200. Nam H-S et al. *Phys. Rev. Lett.* **89** 275502 (2002)
201. Ercolessi F, Andreoni W, Tosatti E *Phys. Rev. Lett.* **66** 911 (1991)
202. Cleveland C L, Luedtke W D, Landman U *Phys. Rev. B* **60** 5065 (1999)
203. Cleveland C L, Luedtke W D, Landman U *Phys. Rev. Lett.* **81** 2036 (1998)
204. Fielicke A et al. *Phys. Rev. Lett.* **93** 023401 (2004)
205. Fielicke A, von Helden G, Meijer G *Eur. Phys. J. D* **34** 83 (2005)
206. Gruene P et al. *Science* **321** 674 (2008)
207. Smalley R E *Laser Chem.* **2** 167 (1983)
208. Hopkins J B et al. E *J. Chem. Phys.* **78** 1627 (1983)
209. Liu Y et al. *J. Chem. Phys.* **85** 7434 (1986)
210. von Helden G et al. *J. Chem. Phys.* **95** 3835 (1991)
211. Jarrold M F, Constant V A *Phys. Rev. Lett.* **67** 2994 (1991)
212. Jarrold M F, Bower J E *J. Chem. Phys.* **96** 9180 (1992)
213. Jarrold M F, Bower J E *J. Chem. Phys.* **98** 2399 (1993)
214. Hunter J M et al. *Phys. Rev. Lett.* **73** 2063 (1994)
215. Shvartsburg A A, Jarrold M F *Phys. Rev. A* **60** 1235 (1999)
216. Shvartsburg A A, Jarrold M F *Phys. Rev. Lett.* **85** 2530 (2000)
217. Schmidt M, Haberland H *C.R. Physique* **3** 327 (2002)
218. Joshi K, Kanhere D G, Blundell S A *Phys. Rev. B* **67** 235413 (2003)
219. Breaux G A et al. *Phys. Rev. Lett.* **91** 215508 (2003)
220. Chasko S et al. *Phys. Rev. Lett.* **92** 135506 (2004)
221. Joshi K, Krishnamurty S, Kanhere D G *Phys. Rev. Lett.* **96** 135703 (2006)
222. Judai K et al. *Int. J. Mass Spectrom.* **229** 99 (2003)
223. Judai K et al. *J. Am. Chem. Soc.* **126** 2732 (2004)
224. Moseler M, Häkkinen H, Landman U *Phys. Rev. Lett.* **89** 176103 (2002)
225. Rainer D R et al. *J. Catal.* **167** 234 (1997)
226. Piccolo L, Henry C R *Appl. Surf. Sci.* **162 – 163** 670 (2000)
227. Piccolo L, Henry C R *J. Mol. Catal. A* **167** 181 (2001)
228. Herzing A A et al. *Science* **321** 1331 (2008)
229. Tian N et al. *Science* **316** 732 (2007)
230. Zhang J et al. *Science* **315** 220 (2007)
231. Winther-Jensen B et al. *Science* **321** 671 (2008)